iScience

CellPress
OPEN ACCESS

Article

Single-cell analysis of immune cells on gingiva-derived mesenchymal stem cells in experimental autoimmune uveitis

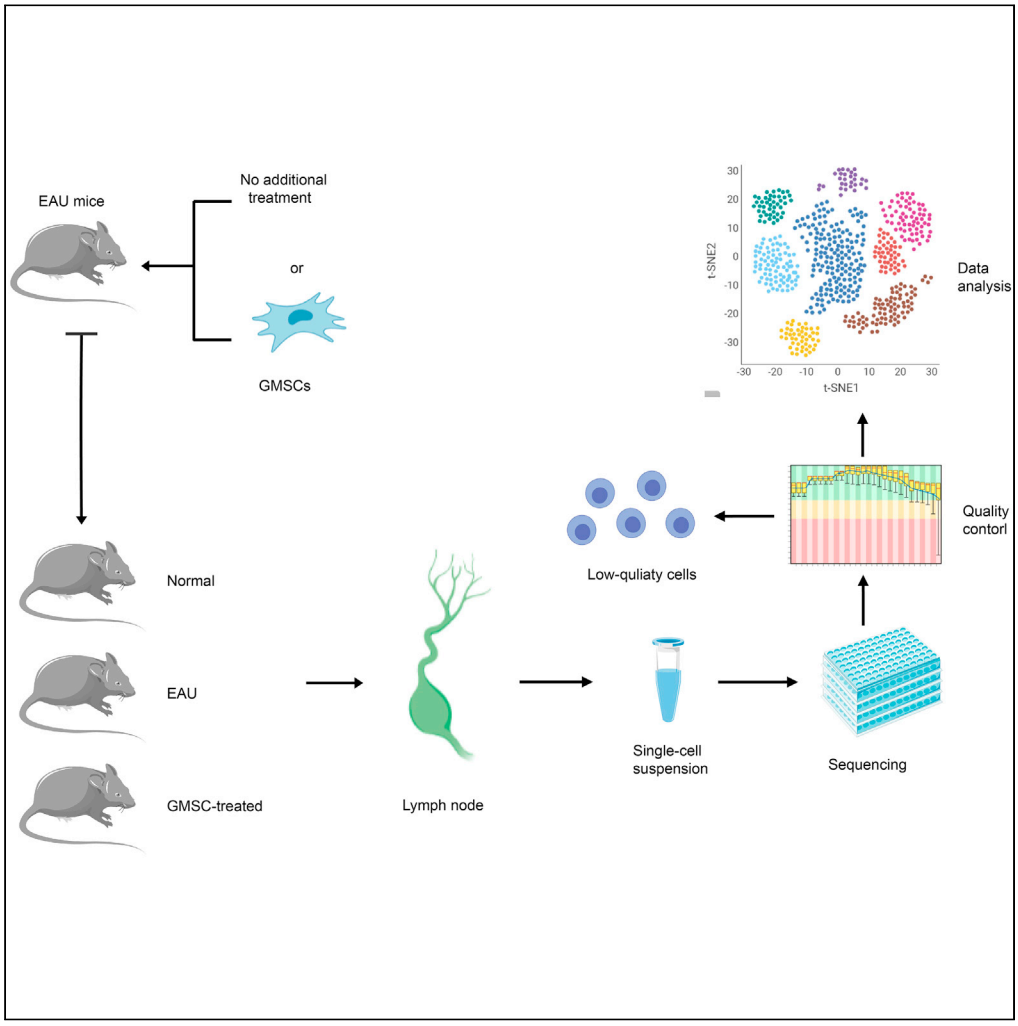

Yuehan Gao, Runping Duan, He Li, ..., Songguo Zheng, Xianchai Lin, Wenru Su

xianchai.lin@qq.com (X.L.)
suwr3@mail.sysu.edu.cn (W.S.)

Highlights

Single-cell RNA sequencing reveals immunosuppressive properties of GMSCs in EAU mice

GMSCs rescue the proportion of Th17 cells and increased the proportion of Treg cells

GMSCs suppress formation of the highly inflammatory $CCR6^{-}CCR2^{+}$ Th17 phenotype

GMSCs show more specific immunosuppressive effect than glucocorticoids in EAU mice

Gao et al., iScience 26, 106729
May 19, 2023
https://doi.org/10.1016/j.isci.2023.106729

iScience

CellPress
OPEN ACCESS

Article

Single-cell analysis of immune cells on gingiva-derived mesenchymal stem cells in experimental autoimmune uveitis

Yuehan Gao,[1,3] Runping Duan,[1,3] He Li,[1,3] Loujing Jiang,[1,3] Tianyu Tao,[1,3] Xiuxing Liu,[1] Lei Zhu,[1] Zhaohuai Li,[1] Binyao Chen,[1] Songguo Zheng,[2] Xianchai Lin,[1,*] and Wenru Su[1,4,*]

SUMMARY

Gingiva-derived mesenchymal stem cells (GMSCs) have shown astonishing efficacy in the treatment of various autoimmune diseases. However, the mechanisms underlying these immunosuppressive properties remain poorly understood. Here, we generated a lymph node single-cell transcriptomic atlas of GMSC-treated experimental autoimmune uveitis mice. GMSC exerted profound rescue effects on T cells, B cells, dendritic cells, and monocytes. GMSCs rescued the proportion of T helper 17 (Th17) cells and increased the proportion of regulatory T cells. In addition to globally altered transcriptional factors (Fosb and Jund), we observed cell type-dependent gene regulation (e.g., Il17a and Rac1 in Th17 cells), highlighting the GMSCs' cell type-dependent immunomodulatory capacity. GMSCs strongly influenced the phenotypes of Th17 cells, suppressing the formation of the highly inflammatory CCR6-CCR2+ phenotype and enhancing the production of interleukin (IL) −10 in the CCR6+CCR2+ phenotype. Integration of the glucocorticoid-treated transcriptome suggests a more specific immunosuppressive effect of GMSCs on lymphocytes.

INTRODUCTION

Mesenchymal stem cells (MSCs) are multipotent progenitor cells with immunosuppressive properties. Stimulated by multiple inflammatory factors, MSCs suppress T and B cells, natural killer (NK) cells, dendritic cell (DC) proliferation, and DC maturation.[1–3] The immunosuppressive properties of MSCs provide a basis for their use in autoimmune disease treatment.[4–6] More recently, our group developed gingiva-derived mesenchymal stem cells (GMSCs), and provided a readily accessible and expandable source of GMSCs with a less surgical technique.[7] Similar to bone marrow-derived MSCs, GMSCs express stem cell-specific marker genes and mesenchymal surface markers, possess *in vitro* multipotent differentiation abilities, and exhibit *in vivo* self-renewal and differentiation capacities. More importantly, GMSCs possess immunosuppressive and anti-inflammatory functions on multiple types of immune cells, whereas they are simultaneously homogeneous and non-tumorigenic.[8–10] Accumulating evidence suggests the benefits of GMSCs in controlling arthritis, oral mucositis, and experimental colitis, endowing GMSCs with immunomodulatory therapeutic potentials for various autoimmune and inflammatory diseases.

For decades, investigations of the immunomodulatory properties of MSCs have shown encouraging outcomes in autoimmune diseases, stimulating the development of MSC-based immunosuppressive strategies.[11,12] Moreover, MSC-mediated immune modulation is cross reactive between species because of their low immunogenicity. Thus, the effectiveness of human MSCs can be evaluated in multiple animal models, including mouse models of experimental colitis, arthritis, and inflammatory bowel disease.[13,14] However, the mechanisms underlying the immunomodulatory properties and the impact of MSCs on the immune system in autoimmune conditions remain poorly understood. Therefore, a comprehensive assessment of the mechanisms responsible for the immunosuppressive effects of MSCs is required.

Autoimmune uveitis (AU), which involves pigmented vascular structures of the eye, is one of the main causes of preventable blindness.[15] In AU conditions, ocular antigens leaking from eyes are absorbed by DCs and presented to autoreactive T cells in lymph nodes (LNs), triggering an aberrant, uncontrolled, and overexuberant T cell-mediated host immune response, whereas B cells also contribute to antigen

[1]State Key Laboratory of Ophthalmology, Zhongshan Ophthalmic Center, Sun Yat-sen University, Guangzhou, Guangdong 51000, China

[2]The Third Affiliated Hospital, Sun Yat-sen University, Guangzhou, Guangdong 51000, China

[3]These authors contributed equally

[4]Lead contact

*Correspondence: xianchai.lin@qq.com (X.L.), suwr3@mail.sysu.edu.cn (W.S.)

https://doi.org/10.1016/j.isci.2023.106729

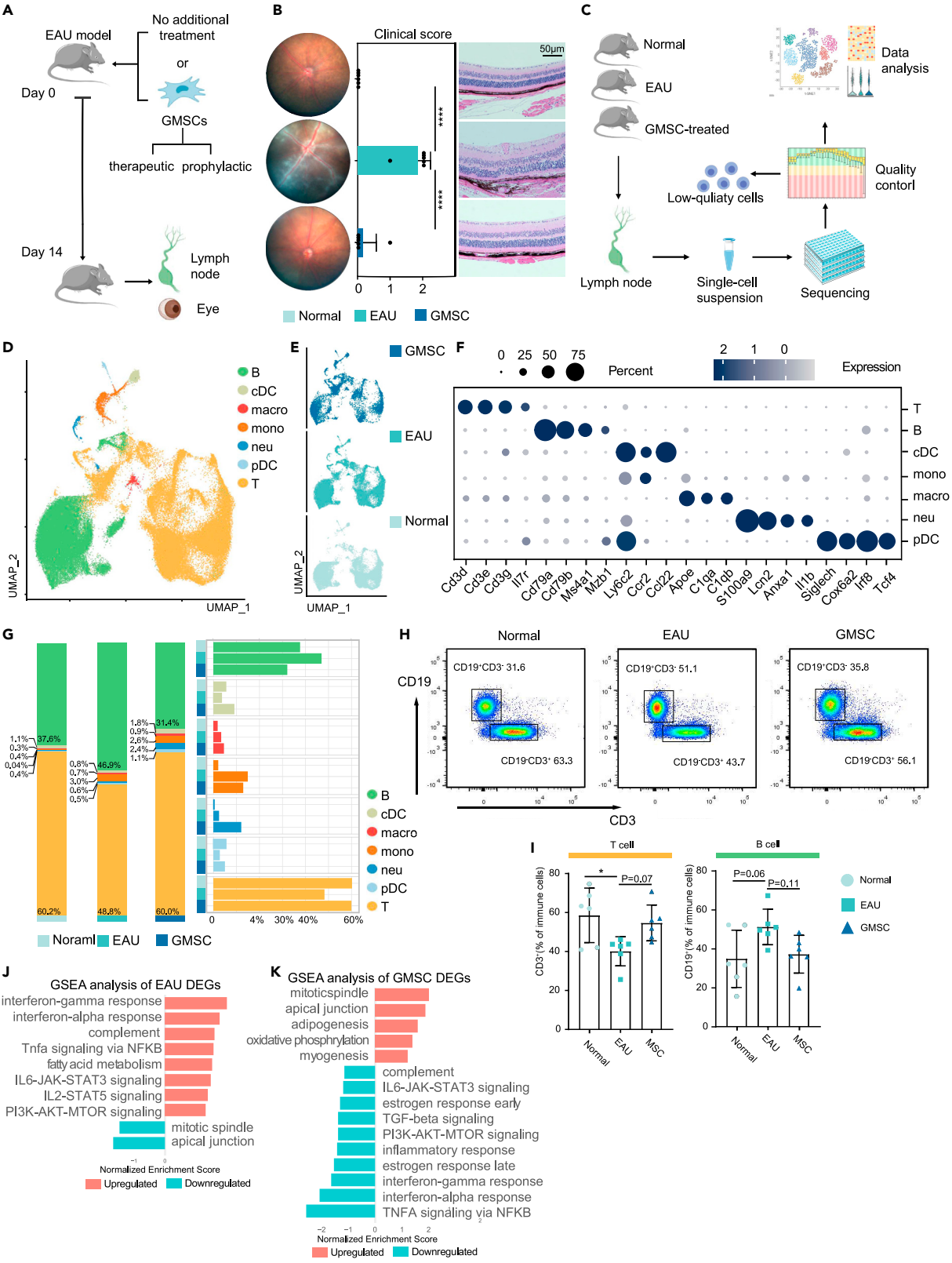
A
EAU model
No additional treatment
or
GMSCs
therapeutic prophylactic
Day 0
Day 14
Lymph node
Eye
B
Clinical score
50μm
Normal EAU GMSC
C
Normal
EAU
GMSC-treated
Data analysis
Quality contorl
Low-quliaty cells
Lymph node
Single-cell suspension
Sequencing
D
B
cDC
macro
mono
neu
pDC
T
UMAP_2
UMAP_1
E
GMSC
EAU
Normal
F
Percent
Expression
Cd3d Cd3e Cd3g Il7r Cd79a Cd79b Ms4a1 Mzb1 Ly6c2 Ccr2 Ccl22 Apoe C1qa C1qb S100a9 Lcn2 Anxa1 Il1b Siglech Cox6a2 Irf8 Tcf4
G
Noraml EAU GMSC
H
Normal
EAU
GMSC
CD19
CD3
CD19+CD3- 31.6
CD19-CD3+ 63.3
CD19+CD3- 51.1
CD19-CD3+ 43.7
CD19+CD3- 35.8
CD19-CD3+ 56.1
I
T cell
B cell
P=0.07
P=0.06
P=0.11
Normal EAU MSC
J
GSEA analysis of EAU DEGs
interferon-gamma response
interferon-alpha response
complement
Tnfa signaling via NFKB
fatty acid metabolism
IL6-JAK-STAT3 signaling
IL2-STAT5 signaling
PI3K-AKT-MTOR signaling
mitotic spindle
apical junction
Normalized Enrichment Score
Upregulated Downregulated
K
GSEA analysis of GMSC DEGs
mitoticspindle
apical junction
adipogenesis
oxidative phosphorylation
myogenesis
complement
IL6-JAK-STAT3 signaling
estrogen response early
TGF-beta signaling
PI3K-AKT-MTOR signaling
inflammatory response
estrogen response late
interferon-gamma response
interferon-alpha response
TNFA signaling via NFKB
Normalized Enrichment Score
Upregulated Downregulated

Figure 1. Study design and clustering of CDLN immune cells by scRNA-seq

(A) Study design. CDLNs of EAU mice, GMSCs-treated EAU mice (therapeutic group), and normal controls were utilized. GMSC, gingiva-derived mesenchymal stem cell.

(B) Left: fundus photography of three groups of mice. Middle: Bar plots of the clinical scores of three groups of mice. Mean +SD with individual values is presented. Data are sampled from six mice per group. Right: Histological assessment of the retina in three groups of mice. Retinal sections were stained with hematoxylin and eosin, and evaluated for histological damage on day 14. Representative H&E staining images of three groups of mice (six mice per group) were presented. p-values are generated by one-way ANOVA. ****$p < 0.0001$. Normal, normal subject; EAU, experimental autoimmune uveitis mouse; GMSC, GMSC-treated (therapeutic) mouse group.

(C) Design of the scRNA-seq and data processing. CDLNs were mixed samples of three groups of mice. A total of six mixed samples (three samples from normal controls, two samples from EAU mice, one sample from GMSC-treated mice) were sequenced without pre-selection of flow cytometry.

(D) UMAP embedding of CDLN immune cells colored by cell types. B, B cell; cDC, conventional dendritic cell; macro, macrophage; mono, monocytes; neu, neutrophil; pDC, plasmacytoid dendritic cell; T, T cell.

(E) UMAP embeddings of lymph node immune cells colored by origins.

(F) Dot plots depict marker gene expression of each cell type. Abbreviations were the same as (D).

(G) Barplots of cell type proportions of seven types of immune cells.

(H) Flow cytometry and quantification of T and B cells (gate on $CD45^+$ immune cells). CD3 staining represents T cells, and CD19 staining represents B cells.

(I) Left: Barplots of proportion of T cells of three groups of mice in CDLNs; Right: Barplots of proportion of B cells of three groups of mice in CDLNs. Mean $\pm$ SD with individual values is presented. Data are sampled from six mice per group. p-values are exact two-sided generated by one-way ANOVA. N, not significant, *$p < 0.05$, **$p < 0.01$, ***$p < 0.001$, ****$p < 0.0001$.

(J) GSEA analysis of upregulated/downregulated EAU DEGs across all CDLN cells.

(K) GSEA analysis of upregulated/downregulated GMSC DEGs across all CDLN cells.

presentation and subsequent T cell activation. Moreover, T helper 17 (Th17) cells are involved in autoimmune uveitis pathogenesis as uveitogenic effectors, and a higher proportion of Th17 cells in the ocular inflammatory infiltrate is related to more severe uveitis.[16–18] Cervical draining LNs (CDLNs) are among the principal draining LNs of the eye and are thus suitable for studying AU pathogenesis and revealing immune alterations by multiple treatments.[19] Currently, glucocorticoids (GCs) remain the forefront immunosuppressive treatment for AU patients, despite the occurrence of multiple side effects and GC resistance.[20] Thus, development of more specific therapeutic approaches is needed.

To determine the effect of GMSCs in AU cases, we generated an experimental autoimmune uveitis (EAU) mouse model, separated CDLNs in normal, EAU, and GMSC-treated mice, and conducted single-cell RNA sequencing (scRNA-seq). The study depicted the effects of GMSCs based on cell type-dependent gene regulation and cell type composition, showed a widespread rescue effect of GMSCs, and indicated that GMSCs strongly influenced Th17 cell phenotypes. Further integration of and comparison with data from prednisone-treated EAU mice from our previous study highlighted the more specific immunosuppressive effects of GMSCs.[21] Our results reveal the transcriptional alterations of immune landscape at the single-cell level after GMSC treatment.

RESULTS

Construction of CDLN single-cell atlases of normal, EAU, and GMSC-treated EAU mice

We generated EAU mouse models by immunizing animals with interphotoreceptor retinoid-binding protein (IRBP), and used normal mice as controls. To investigate the effect of GMSCs, EAU mice were evenly matched and randomized into three groups: EAU group without additional treatment, prophylactic group (treated with GMSCs at day 0), and therapeutic group (treated at day 7) (Figures 1A and S1A). To confirm the identity of the GMSCs, we performed flow cytometry. Based on previous studies, we characterized GMSCs using surface markers, including CD14, CD29, HLA-DR, CD39, CD105, CD73, CD90, CD44, CD34, and CD45 (Figure S1B).

After 14 days, we observed increased clinical scores and inflamed fundus of EAU mice, and performed histological examination. We found that two different GMSC treatment therapies (prophylactic and therapeutic) reversed these effects, showing the promising efficacy of GMSCs in disease remission (Figures 1B and S2A). Histological examination indicated massive inflammatory cell infiltration throughout the retina, disorganized choroidal structures, and diffuse retinal edema in EAU mice, which were profoundly reversed by GMSC treatment (Figure 1B). To better explore the underlying mechanisms of action of GMSCs, we focused on the prophylactic group that exhibited stronger rescue effects based on clinical scores and fundus photography.

We first developed single-cell RNA transcriptional profiles of CDLNs of approximately 71,000 high-quality cells from the three groups of mice (Figure 1C). For scRNA-seq, we included three samples from normal

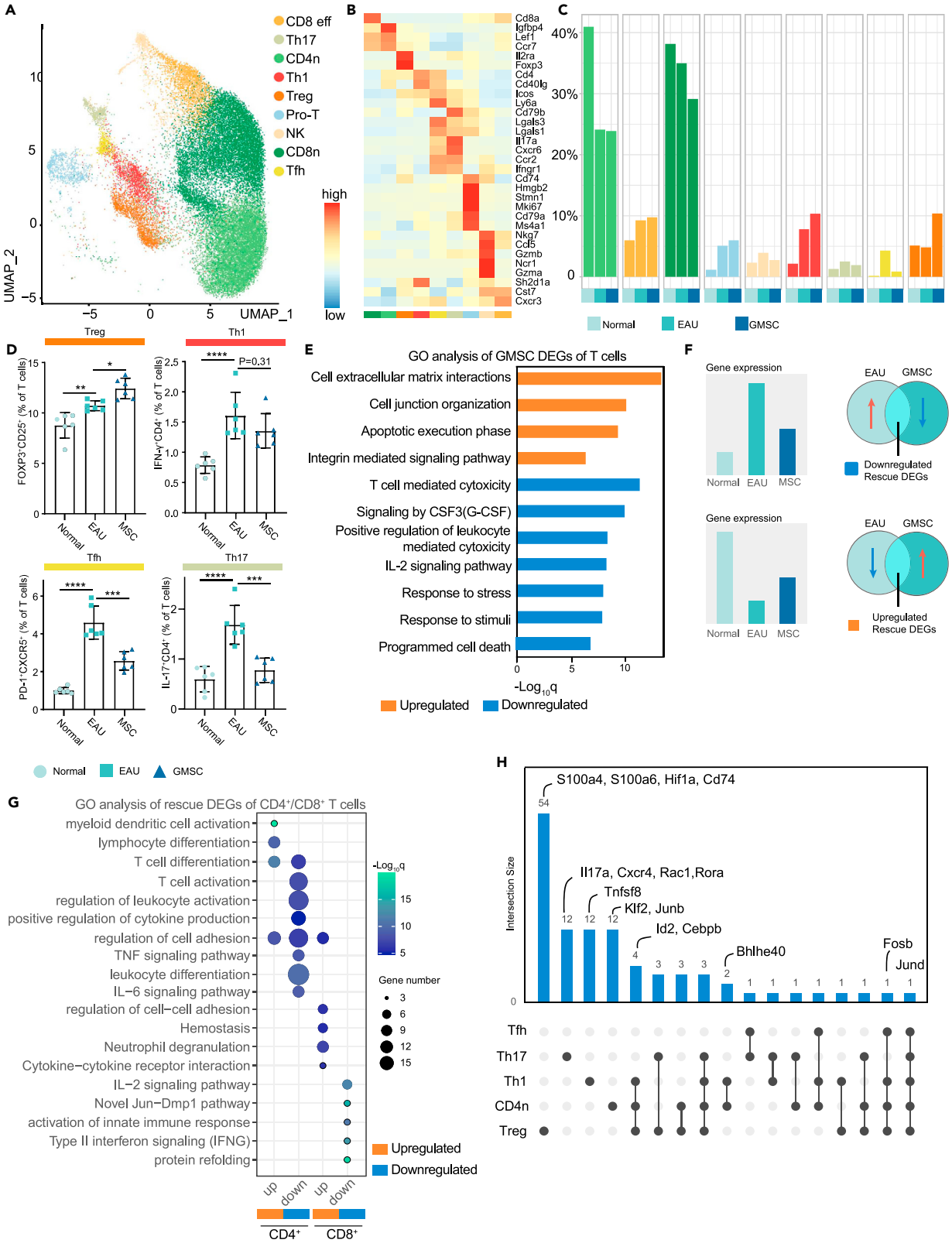
A
CD8 eff
Th17
CD4n
Th1
Treg
Pro-T
NK
CD8n
Tfh
UMAP_2
UMAP_1
B
high
low
Cd8a
Igfbp4
Lef1
Ccr7
Il2ra
Foxp3
Cd4
Cd40lg
Icos
Ly6a
Cd79b
Lgals3
Lgals1
Il17a
Cxcr6
Ccr2
Ifngr1
Cd74
Hmgb2
Stmn1
Mki67
Cd79a
Ms4a1
Nkg7
Cd5
Gzmb
Ncr1
Gzma
Sh2d1a
Cst7
Cxcr3
C
40%
30%
20%
10%
0
Normal
EAU
GMSC
D
Treg
Th1
Tfh
Th17
FOXP3+CD25+ (% of T cells)
IFN-γ+CD4+ (% of T cells)
PD-1+CXCR5+ (% of T cells)
IL-17+CD4+ (% of T cells)
P=0.31
Normal
EAU
MSC
Normal
EAU
GMSC
E
GO analysis of GMSC DEGs of T cells
Cell extracellular matrix interactions
Cell junction organization
Apoptotic execution phase
Integrin mediated signaling pathway
T cell mediated cytoxicity
Signaling by CSF3(G-CSF)
Positive regulation of leukocyte mediated cytoxicity
IL-2 signaling pathway
Response to stress
Response to stimuli
Programmed cell death
-Log10q
Upregulated
Downregulated
F
Gene expression
Normal
EAU
MSC
EAU
GMSC
Downregulated Rescue DEGs
Gene expression
Normal
EAU
MSC
EAU
GMSC
Upregulated Rescue DEGs
G
GO analysis of rescue DEGs of CD4+/CD8+ T cells
myeloid dendritic cell activation
lymphocyte differentiation
T cell differentiation
T cell activation
regulation of leukocyte activation
positive regulation of cytokine production
regulation of cell adhesion
TNF signaling pathway
leukocyte differentiation
IL−6 signaling pathway
regulation of cell−cell adhesion
Hemostasis
Neutrophil degranulation
Cytokine−cytokine receptor interaction
IL−2 signaling pathway
Novel Jun−Dmp1 pathway
activation of innate immune response
Type II interferon signaling (IFNG)
protein refolding
-Log10q
Gene number
Upregulated
Downregulated
up
down
up
down
CD4+
CD8+
H
S100a4, S100a6, Hif1a, Cd74
Il17a, Cxcr4, Rac1,Rora
Tnfsf8
Klf2, Junb
Id2, Cebpb
Bhlhe40
Fosb
Jund
Intersection Size
Tfh
Th17
Th1
CD4n
Treg

Figure 2. GMSCs exerted immunosuppressive effect on T cell subsets of EAU mice

(A) UMAP embeddings of T cell subtypes. CD8 eff: $CD8^+$ effector T cells; Th17: Th17 cells; CD4n: $CD4^+$ naive T cells; Th1: Th1 cells; Treg: regulatory T cells; Pro-T: proliferating T cells; NK: NK cells; CD8n: $CD8^+$ naive T cells; Tfh: follicular T cells.

(B) Heatmap of marker genes of T cell subtypes in three groups of mice.

(C) Barplots of cell proportions of T cell subtypes. Annotation colors were the same as (A).

(D) Barplots of cell proportions of Treg (gate on $CD4^+$T cells), Th1, Tfh (gate on $CD4^+B220^-$T cells) and Th17 cells. Mean ± SD with individual values is presented. Data are sampled from six mice per group. p-values are exact two-sided generated by one-way ANOVA. N, not significant, *p< 0.05, **p< 0.01, ***p< 0.001, ****p< 0.0001.

(E) GO analysis of upregulated/downregulated GMSC DEGs of all T cells.

(F) Schematic diagram of upregulated/downregulated rescue DEGs.

(G) GO analysis of upregulated/downregulated DEGs in $CD4^+$/$CD8^+$T cells.

(H) Venn diagram of commonly/specifically downregulated rescue DEGs among five types of $CD4^+$T cells. The black dot at the bottom of the diagram indicates that genes were downregulated in certain $CD4^+$T cell subset(s). The number over each bar indicates the overall counts of commonly/specifically downregulated genes in certain T cell subset(s).

controls, two samples from EAU mice, and one sample from GMSC-treated mice (each sample was mixed with CDLNs from three mice). Based on marker gene expression (detailed in STAR Methods), seven immune cell types were identified: (1) T cells, (2) B cells, (3) monocytes, (4) macrophages, (5) neutrophils, (6) plasmacytoid dendritic cells (pDCs), and (7) conventional dendritic cells (cDCs) (Figures 1D–1F and S2B). Regarding cell type proportions, our single-cell data suggested that GMSC treatment exerted a profound rescue effect on the proportions of T cells, B cells, cDCs, and pDC, suggesting the immunosuppressive properties of GMSCs (Figure 1G). Moreover, GMSC treatment increased the proportions of macrophages and neutrophils. By validating the proportion of T and B cells by flow cytometry, we found that the proportion of T cells was rescued by GMSC treatment, and similar trends were observed for the rescued proportion of B cells (Figures 1H and 1I).

To characterize global transcriptional changes, we identified differentially expressed genes (DEGs) between normal and EAU mice (EAU DEGs), and between EAU and GMSC-treated EAU mice (GMSC DEGs). GSEA analysis of all cell types indicated that multiple cytokine-associated pathways were enhanced in the EAU model and suppressed in the GMSC-treated EAU mice (Figures 1J and 1K). Overall, we constructed a transcriptional atlas of CDLNs to provide a basis for investigating the mechanisms of action of GMSCs.

Immunosuppressive effect of GMSCs on T cell subsets

To further analyze the T cell subsets, T cells were subdivided into nine subpopulations: (1) $CD4^+$ naive T cells, (2) T helper 1 (Th1) cells, (3) Th17 cells, (4) proliferating T cells, (5) NK cells, (6) follicular T (Tfh) cells, (7) $CD8^+$ naive T cells, (8) $CD8^+$ effector T cells and (7) regulatory T (Treg) cells (Figure 2A). Identification of T cell subpopulations was based on marker gene expression described in previous studies (Figures 2B and S2C, marker genes detailed in STAR Methods). Th1 and Tfh clusters were further distinguished based on their marker genes (Figures S2D–S2F). Next, we investigated the changes in T cell subpopulations in normal, EAU, and GMSC-treated EAU mice. Notably, based on scRNA-seq data, GMSC treatment exerted a profound rescue effect on the proportions of Th17, Tfh, and NK cells, and elevated Treg proportions (Figure 2C). We also found that the proportion of $CD4^+$ naive T cells and $CD8^+$ naive T cells was further suppressed by GMSC treatment (Figure 2C). To validate our findings, we performed flow cytometry to explore the proportion of T cell subtypes. Of interest, flow cytometry validation indicated that the proportion of Th17 and Tfh cells increased in EAU mice and was rescued by GMSC treatment (Figures 2D and S3A). The similar trend was also observed in Th1 cells. Furthermore, we found that the proportion of Tregs was increased in EAU mice, which was further increased by GMSC treatment. We inferred that these cell types play a central role in the action of GMSCs.

To obtain a global view of the transcriptomic changes in T cells after GMSC treatment, overall transcriptomic alterations across all T cell subsets were defined. GO analysis suggested that upregulated GMSC DEGs were enriched in cell-junction-associated pathways, whereas downregulated GMSC DEGs were enriched in function-associated pathways including "Signaling by CSF3," "T cell mediated cytoxicity" and "IL-2 signaling pathway," indicating that GMSCs could suppress T cell functions by inhibiting multiple pathways (Figure 2E).

GMSCs partially reversed the effects of EAU in $CD4^+$T cells

Based on the EAU/GMSC DEGs, we defined two types of "rescue DEGs," upregulated or downregulated, which refer to EAU DEGs exhibiting contrasting regulatory tendencies after GMSC treatment (Figure 2F).

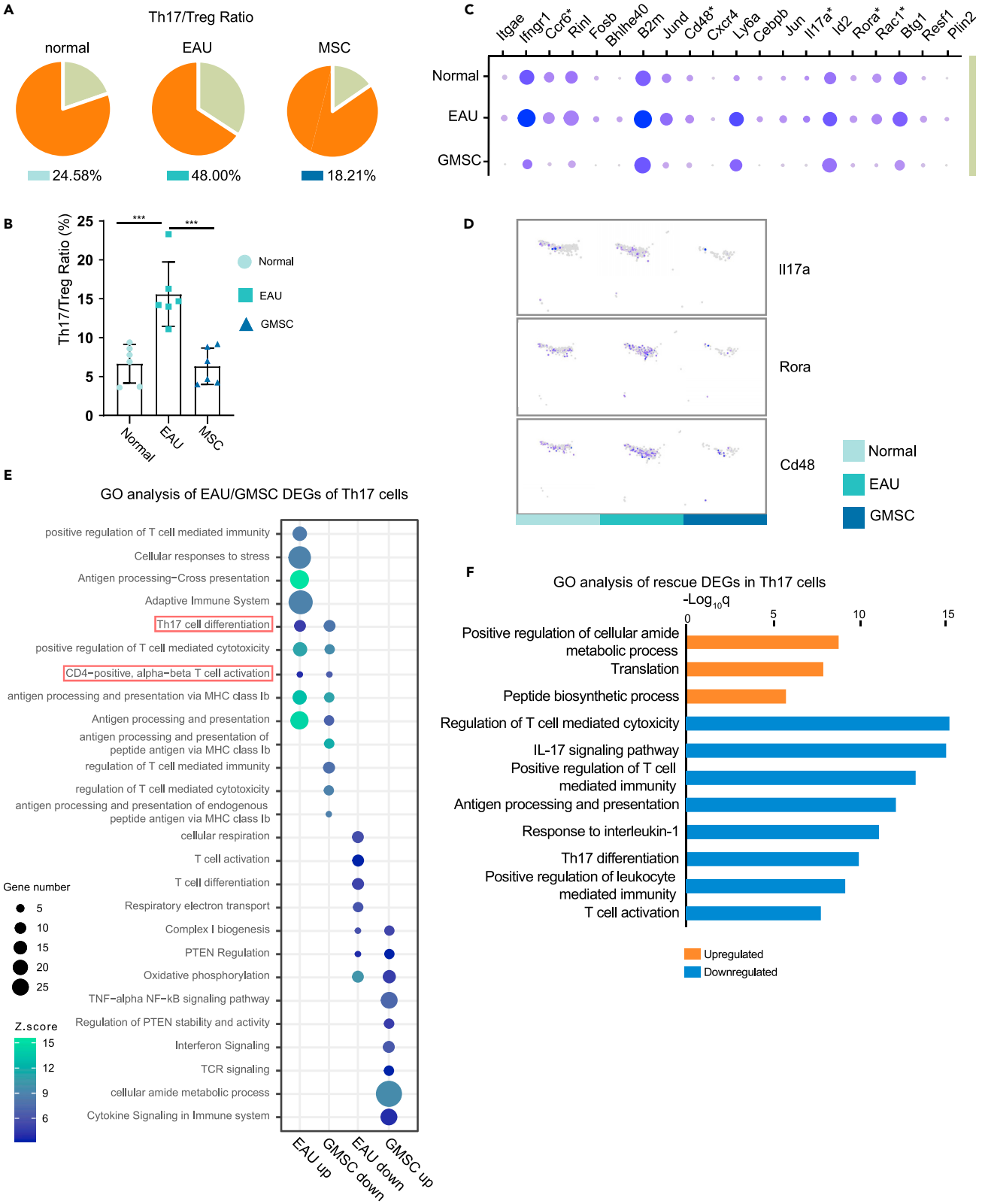
A
Th17/Treg Ratio
normal
EAU
MSC
24.58%
48.00%
18.21%
B
Th17/Treg Ratio (%)
25
20
15
10
5
0
***
***
Normal
EAU
GMSC
Normal
EAU
MSC
C
Itgae
Ifngr1
Ccr6*
Rinl
Fosb
Bhlhe40
B2m
Jund
Cd48*
Cxcr4
Ly6a
Cebpb
Jun
Il17a*
Id2
Rora*
Rac1*
Btg1
Resf1
Plin2
Normal
EAU
GMSC
D
Il17a
Rora
Cd48
Normal
EAU
GMSC
E
GO analysis of EAU/GMSC DEGs of Th17 cells
positive regulation of T cell mediated immunity
Cellular responses to stress
Antigen processing−Cross presentation
Adaptive Immune System
Th17 cell differentiation
positive regulation of T cell mediated cytotoxicity
CD4−positive, alpha−beta T cell activation
antigen processing and presentation via MHC class Ib
Antigen processing and presentation
antigen processing and presentation of peptide antigen via MHC class Ib
regulation of T cell mediated immunity
regulation of T cell mediated cytotoxicity
antigen processing and presentation of endogenous peptide antigen via MHC class Ib
cellular respiration
T cell activation
T cell differentiation
Respiratory electron transport
Complex I biogenesis
PTEN Regulation
Oxidative phosphorylation
TNF−alpha NF−kB signaling pathway
Regulation of PTEN stability and activity
Interferon Signaling
TCR signaling
cellular amide metabolic process
Cytokine Signaling in Immune system
Gene number
5
10
15
20
25
Z.score
15
12
9
6
EAU up
GMSC down
EAU down
GMSC up
F
GO analysis of rescue DEGs in Th17 cells
-Log10q
0
5
10
15
Positive regulation of cellular amide metabolic process
Translation
Peptide biosynthetic process
Regulation of T cell mediated cytoxicity
IL-17 signaling pathway
Positive regulation of T cell mediated immunity
Antigen processing and presentation
Response to interleukin-1
Th17 differentiation
Positive regulation of leukocyte mediated immunity
T cell activation
Upregulated
Downregulated

Figure 3. GMSCs partially reversed the effect of EAU in Th17 cells

(A) Pie charts indicate the Th17/Treg ratios in three groups of mice based on scRNA-seq. Ratios are shown under the pie charts. Normal, normal subject; EAU, experimental autoimmune uveitis mouse; GMSC, GMSC-treated mouse group.

(B) Barplots of Th17/Treg ratios in three groups of mice based on flow cytometry. Mean ± SD with individual values is presented. Data are sampled from six mice per group. ***p< 0.001. p-values are generated by one-way ANOVA.

(C) Dot plots of rescue DEGs of GMSCs in Th17 cells.

(D) UMAP embeddings show expression of *Il17a*, *Rora* and *Cd48* of Th17 cells in three groups of mice.

(E) GO analysis of upregulated/downregulated EAU/GMSC DEGs of Th17 cells. EAU up: upregulated EAU DEGs, GMSC down: downregulated GMSC DEGs, EAU down: downregulated EAU DEGs, GMSC up: upregulated GMSC DEGs.

(F) GO analysis of upregulated/downregulated rescue DEGs in Th17 cells.

Next, we analyzed the potential functions of the rescued genes of $CD4^+$ or $CD8^+$T cells. GO analysis suggested enrichment of both upregulated and downregulated rescue DEGs in $CD4^+$T cells in autoimmune-response-associated pathways, including "T cell differentiation," "TNF signaling pathway," "positive regulation of cytokine production," and "IL-17 signaling pathway," whereas enrichment of rescue DEGs in $CD8^+$T cells appeared less specific (Figure 2G). Our findings suggest that GMSCs have profound effects on $CD4^+$T cell differentiation, cytokine production, and Th17 cell differentiation. Given the proportional alterations of the T cell subset, we further performed a trajectory analysis to explore the effects of GMSCs on T cell differentiation. To define the differentiation trajectory more clearly, we have removed NK cells and proliferating T cells before performing trajectory analysis. Of interest, we found that, compared with normal controls, $CD4^+$ naive T cells were inclined to differentiate into Th17 and Tfh cells, whereas $CD8^+$ naive T cells tended to differentiate into effector $CD8^+$T cells (Figures S3B and S3C). Moreover, the differentiation of naive CD4 + cells into Th17 cells was suppressed by GMSC treatment, and GMSCs seemed to improve the generation of Tregs from $CD4^+$ naive T cells.

Next, we investigated the rescue DEGs of the five subtypes of $CD4^+$T cells and generated a Venn diagram to investigate the specificity of rescue DEGs (Figures 2H and S3D). We found that the commonly rescued genes encoded transcription factor (TF) components including *Jund*, *Fosb*, *Cebpb*, and *Id2* (Figure S3E). We identified larger numbers of cell type-specific downregulated rescue DEGs in Tregs and Th17 cells, and upregulated rescue DEGs in Tregs and Th1 cells. Notably, these cell type-specific rescue DEGs included multiple function-associated genes, including *Nrp1* (for Tregs) and *Il17a*, *Rac1*, *Cxcr4* and *Rora* for Th17 cells.[22–24] These results indicated the main role of $CD4^+$T cells, especially Tregs and Th17 cells, in the actions of GMSCs.

GMSCs rescue effects of Th17 cells in EAU mice

Previous studies have revealed that Th17 and Treg cells play major roles in autoimmunity. Comparing the Th17:Treg ratio in the three groups of mice, a strong rescue effect of GMSCs was observed (Figure 3A). Furthermore, we reanalyzed the Th17/Treg ratio based on flow cytometry findings, and found observed similar rescue effect of GMSCs (Figure 3B). Thus, we first focused on Th17 cells, analyzed the EAU, GMSC, and rescue DEGs in the Th17 subset and found a considerable rescue effect of GMSCs on the expression of function-associated genes, including the key cytokine *Il17a*, migration-associated *Cxcr4* and *Ccr6*, and function-associated *Rac1* and *Rora* (Figures 3C and 3D).[23–26] Furthermore, we observed similar functional enrichment between EAU DEGs and GMSC DEGs with contrasting regulatory tendencies (Figure 3E). Enrichment of "Th17 cell differentiation" in downregulated GMSC DEGs suggests a specific rescue effect of GMSCs on Th17 cells. GO analysis of the downregulated rescue DEGs of Th17 cells showed a similar enrichment in IL-17-associated pathways (Figure 3F).

GMSCs inhibit the formation of $CCR6^-CCR2^+$ pathogenetic Th17 cells

Recent studies have revealed two different phenotypes of Th17 cells: (1) less inflammatory IL-10-producing Th17 cells and (2) highly inflammatory granulocyte-macrophage colony-stimulating factor (GM-CSF)-producing Th17 cells.[27–31] Next, we validated the effects of GMSCs on Th17 cells by separating them and evaluating the production of IL-10 and GM-CSF (Figures 4A–4D, S3D, and S4A–S4B). EAU mice produced more GM-CSF and less IL-10 in CDLNs and spleens than normal controls, and GMSC treatment strongly reversed these effects.

Recently, researchers identified GM-CSF-producing Th17 cells bearing a $CCR6^-CCR2^+$ phenotype in mice, whereas the IL-10-producing phenotype is IL-23-driven with the $CCR6^+CCR2^+$ signature, which was also validated in our results (Figure S4C).[32] Furthermore, we observed a strong rescue effect of GMSCs on

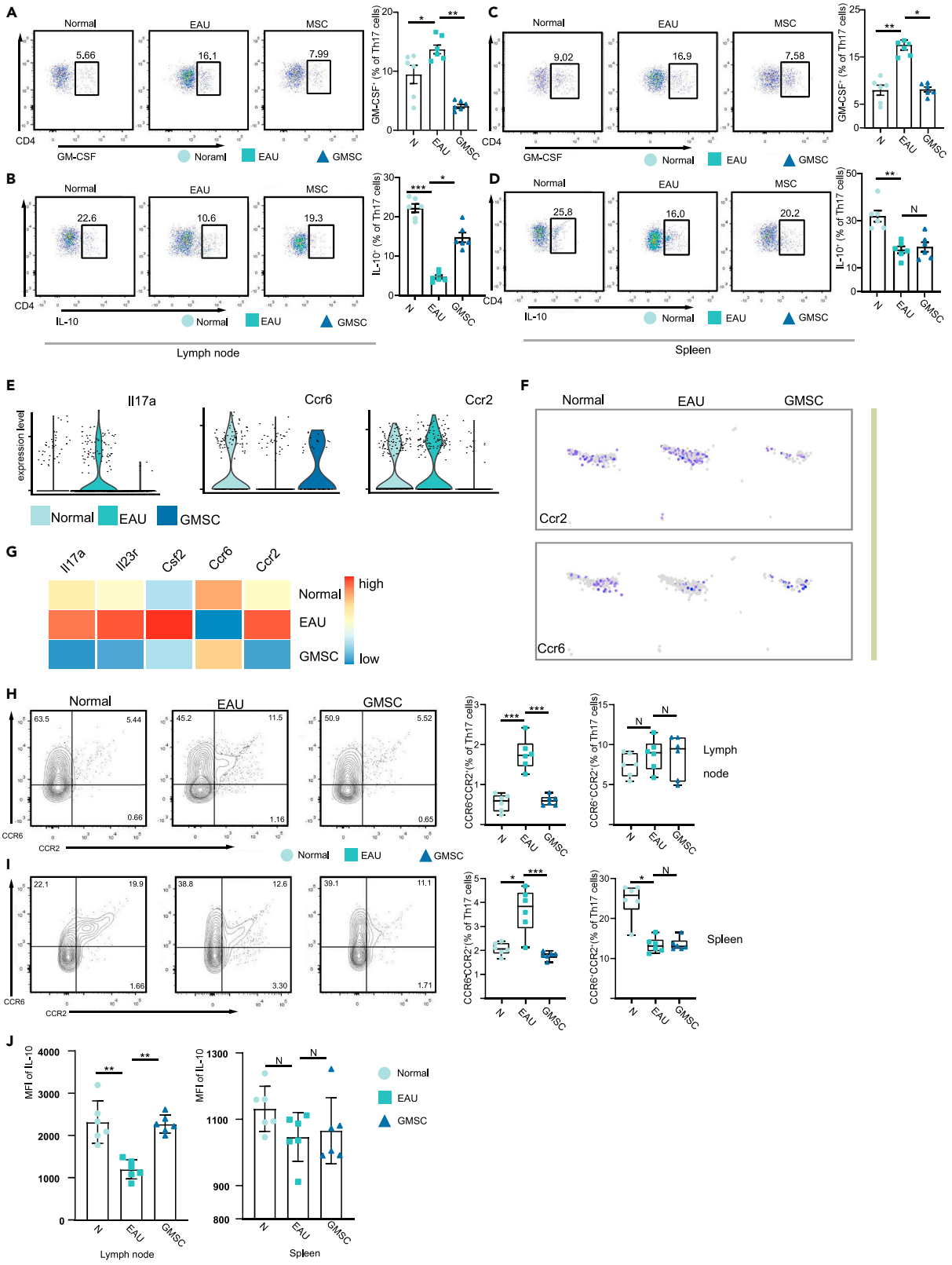
A
Normal
EAU
MSC
5.66
16.1
7.99
CD4
GM-CSF
Noramal
EAU
GMSC
GM-CSF+ (% of Th17 cells)
B
22.6
10.6
19.3
IL-10
IL-10+ (% of Th17 cells)
Lymph node
C
9.02
16.9
7.58
Spleen
D
25.8
16.0
20.2
E
Il17a
Ccr6
Ccr2
expression level
F
G
Il17a
Il23r
Csf2
Ccr6
Ccr2
high
low
H
63.5
5.44
0.66
45.2
11.5
1.16
50.9
5.52
0.65
CCR6
CCR2
CCR6+CCR2+(% of Th17 cells)
Lymph node
I
22.1
19.9
1.66
38.8
12.6
3.30
39.1
11.1
1.71
Spleen
J
MFI of IL-10
Lymph node
Spleen

Figure 4. GMSCs influenced Th17 phenotype formation

(A–D) Left: Flow cytometry and quantification of GM-CSF or IL-10 staining in Th17 cells in lymph nodes (A and C) or spleen (B and D). The percentage of cells was labeled over each gate. Right: Barplots of GM-CSF or IL-10 in Th17 cells across three groups of mice in lymph nodes or spleens. Mean ± SD with individual values is presented. Data are sampled from six mice per group. p-values are exact two-sided generated by one-way ANOVA. N, not significant, *p< 0.05, **p< 0.01, ***p< 0.001, ****p< 0.0001. Normal, normalsubject; EAU, experimental autoimmune uveitis mouse; GMSC, GMSC-treated mouse group.

(E) Violin plots of expression of *Ccr2*, *Ccr6* and *Il17a* of three groups of mice in Th17 cells.

(F) UMAP embeddings of *Ccr2* and *Ccr6* of Th17 cells in three groups of mice.

(G) Heatmap of phenotype-associated genes of Th17 cells in three groups of mice.

(H and I) Left: Flow cytometry of staining of CCR6/CCR2 on Th17 cells in lymph nodes (H) or spleens (I) in three groups of mice. Data are sampled from six mice per group. Right: Bar plots summarize the proportion of $CCR6^{+}CCR2^{-}$, $CCR6^{-}CCR2^{+}$ and $CCR6^{+}CCR2^{+}$ Th17 phenotypes in three groups of mice. Mean ± SD with individual values is presented. Data are sampled from six mice per group. p-values are exact two-sided generated by one-way ANOVA. N, not significant, *p< 0.05, **p< 0.01, ***p< 0.001.

(J) Bar plots of the mean fluorescent index (MFI) of IL-10 staining in $CCR6^{+}CCR2^{+}$ Th17 cells of lymph nodes (left) or spleens (right) in three groups of mice. Mean ± SD with individual values is presented. Data are sampled from six mice per group. p-values are exact two-sided generated by one-way ANOVA. N, not significant, ***p< 0.001, ****p< 0.0001.

the expression of *Ccr2*, *Ccr6*, *Il23r*, and *Csf2* (encoding GM-CSF) in Th17 cells (Figures 4E–4G). Thus, we hypothesized that GMSCs could affect Th17 phenotypes, which might partly account for their immunosuppressive properties.

To validate our hypothesis, we compared the expression of CCR2 and CCR6 in Th17 cells across three types of mice (Figures 4H, 4I, and S4D). Comparing EAU to normal mice, we observed elevated potentially pathologic $CCR6^{-}CCR2^{+}$ Th17 cells in EAU mice. More importantly, GMSCs reversed these effects by decreasing $CCR6^{-}CCR2^{+}$ Th17 cells in GMSC-treated mice.

To assess whether GMSCs affect the inflammatory properties of $CCR6^{+}CCR2^{+}$ Th17 cells, we examined the expression of IL-10 and found decreased IL-10 expression in EAU mice, which was reversed by GMSCs (Figures 4J and S4E). We inferred that EAU conditions and GMSC treatment altered the inflammatory properties of $CCR6^{+}CCR2^{+}$ Th17 cells. Thus, both EAU and GMSC treatments have an impact on the composition and inflammatory properties of Th17 cells.

GMSCs effect on other T cell subtypes

The distinct rescue effects of GMSCs on other T cell types were also explored. We observed high proportions of rescued genes in Tregs and rescued genes associated with Treg function, including *Traf3ip3*, *Nrp1*, and *Pim1*, indicating that GMSCs enhanced Treg function (Figure S5A).[22,33,34] GO analysis of rescue DEGs supported the rescue effect of GMSCs on Tregs, with upregulated rescue DEGs enriched in pathways inhibiting the immune response (Figure S5B).

The results also identified rescue DEGs of other types of T subpopulations and performed a functional enrichment analysis of these genes. Globally, GMSC exhibited immunosuppressive properties on T cell subtypes, with downregulated rescue DEGs enriched in cytokine-related pathways (Figure S5C). The results identified rescued the T cell survival-associated genes *Bcl2* and *Mcl1* in naive $CD4^{+}$T cells (Figure S5D).[35,36] As for Th1 subsets, we found upregulated rescued *Pdcd1* and downregulated rescued *Satb1*, which supported the immunosuppressive properties of GMSCs.[37,38] The expression of several cytokines and chemokine receptors was rescued by GMSCs in proliferative T cells, suggesting that GMSC treatment might weaken T cell migration. GMSCs also rescued the expression of *Cd69*, *Cd74* ($CD8^{+}$ effector T cells), *Ccl3*, and *Gzmb* (NK cells).[39–42]

Next, we analyzed the specificity of rescue DEGs in T cell subtypes and generated Venn diagrams based on the identified DEGs. We identified the largest number of specific downregulated rescue DEGs in Tregs (Figure S5E). Moreover, the data indicated that the expression of TF, *Hif1a*, and the costimulatory molecule *Cd28* specifically downregulated rescue DEGs of Tregs, demonstrating the unique functions of GMSCs on these cells.[43,44]

GMSCs immunosuppressive properties of B and myeloid cells

The effects of GMSCs on B cells and myeloid clusters (cDCs, pDCs, monocytes, macrophages, and neutrophils) in EAU mice was determined, and B cells were subdivided into three subsets (naive, germinal, and plasma) (Figures 5A, 5B, S6A, and S6B).

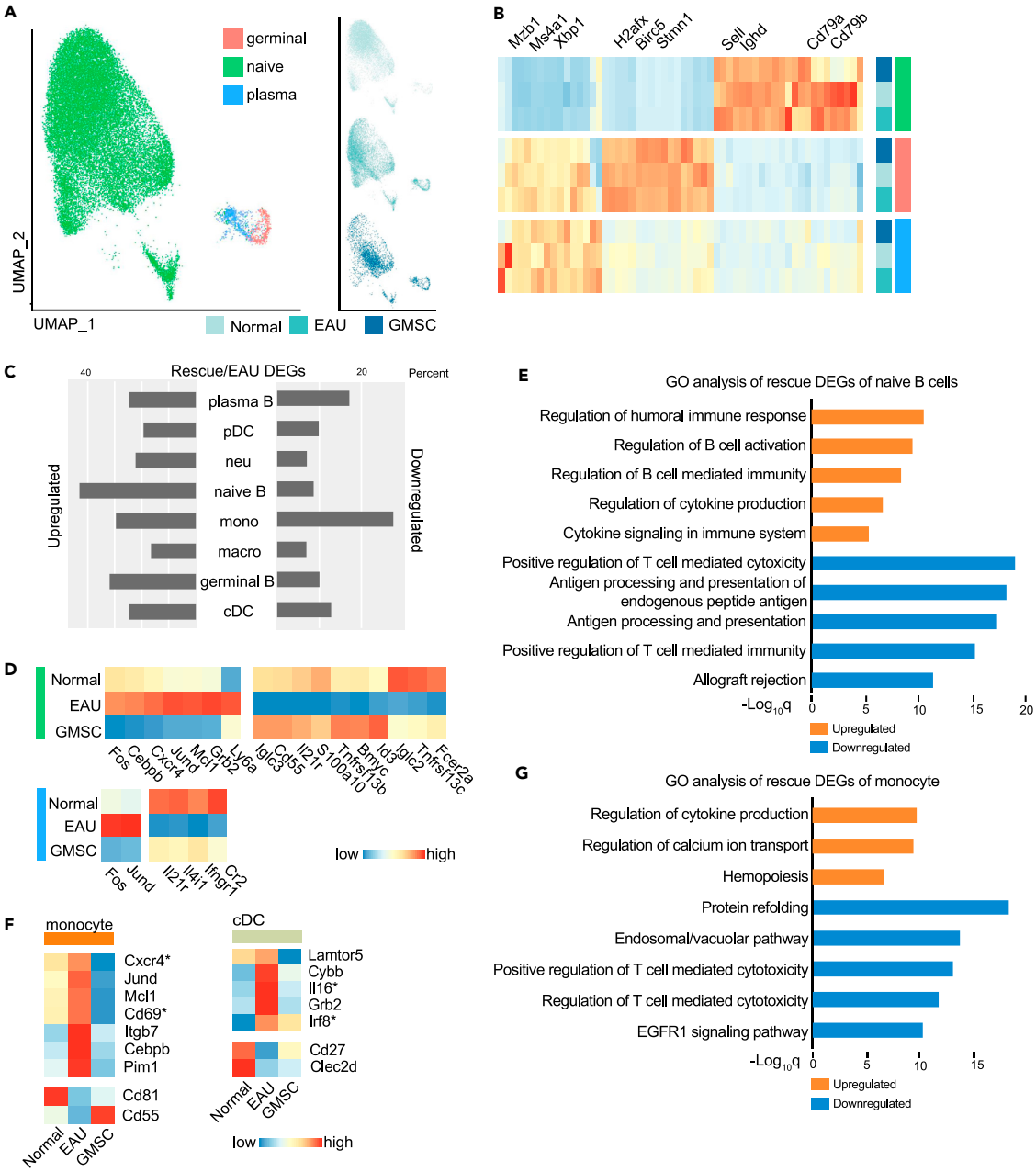

Figure 5. GMSCs influenced B and myeloid cells

(A) UMAP embeddings colored by B cell subtypes (left) or origins (right). Germinal: germinal B cells; naive: naive B cells; plasma: plasma B cells. Normal, normal subject; EAU, experimental autoimmune uveitis mouse; GMSC, GMSC-treated (therapeutic) mouse group.

(B) Heatmap of marker genes of B cell subtypes in three groups of mice.

(C) Bar plots of rescue/EAU DEGs ratios. Left: downregulated rescue DEGs/upregulated EAU DEGs; right: upregulated rescue DEGs/downregulated EAU DEGs.

(D) Heatmap of rescue DEGs of naive B and plasma B cells in three groups of mice.

(E) GO analysis of upregulated/downregulated rescue DEGs of naive B cells.

(F) Heatmap of rescue DEGs in monocytes and cDCs in three groups of mice.

(G) GO analysis of upregulated/downregulated rescue DEGs of monocytes.

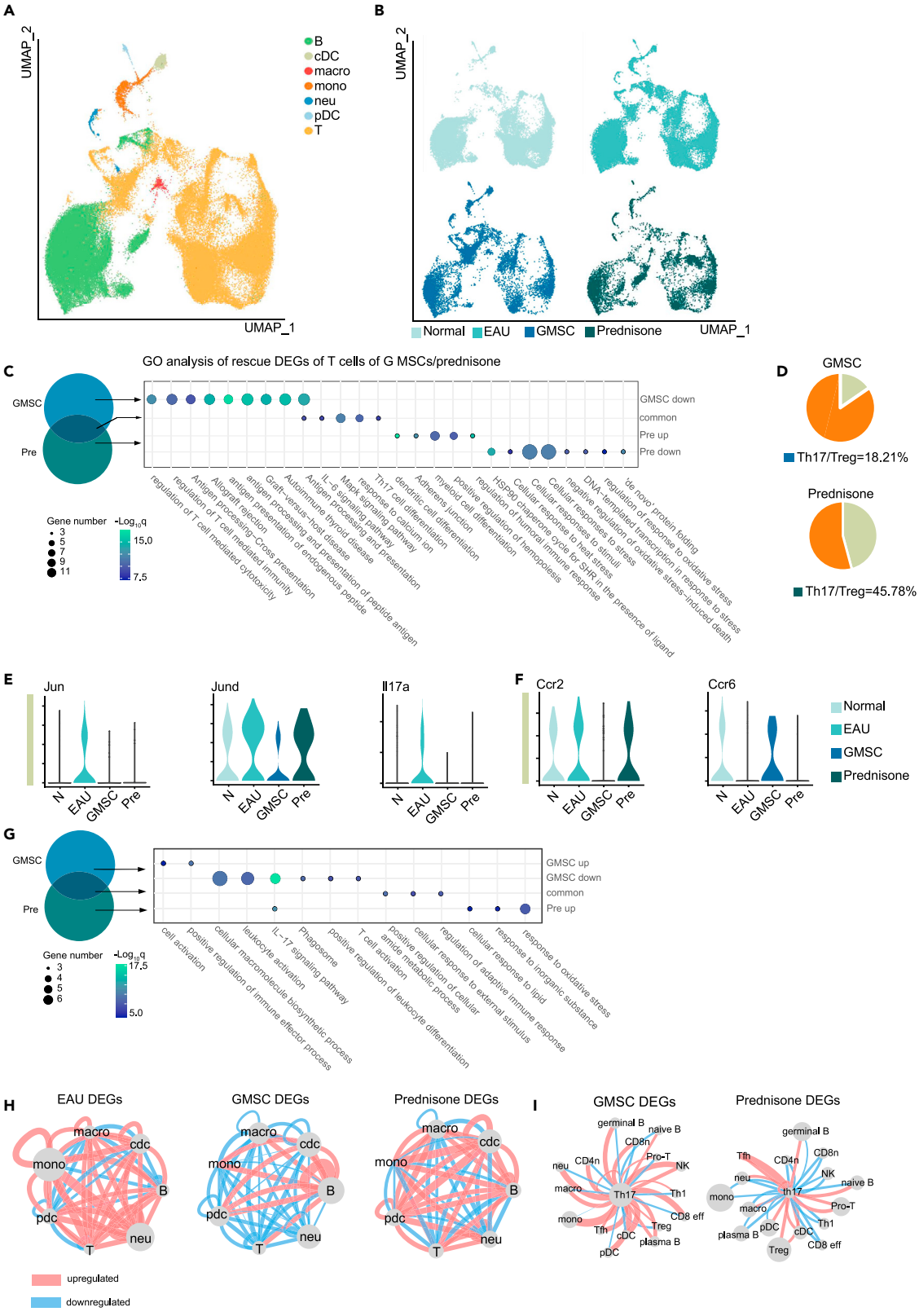
A
UMAP_2
UMAP_1
B
cDC
macro
mono
neu
pDC
T
B
UMAP_2
Normal
EAU
GMSC
Prednisone
UMAP_1
C
GO analysis of rescue DEGs of T cells of G MSCs/prednisone
GMSC
Pre
GMSC down
common
Pre up
Pre down
Gene number
-Log10q
15.0
7.5
regulation of T cell mediated cytotoxicity
regulation of T cell mediated immunity
Antigen processing−Cross presentation
Allograft rejection
antigen presentation of endogenous peptide
Graft−versus−host disease
Autoimmune thyroid disease
antigen processing and presentation
IL−6 signaling pathway
Antigen processing and presentation
Mapk signaling pathway
response to calcium ion
Th17 cell differentiation
dendritic cell differentiation
Adherens junction
myeloid cell differentiation
positive regulation of hemopoiesis
regulation of humoral immune response
HSP90 chaperone cycle for SHR in the presence of ligand
Cellular response to heat stress
Cellular responses to stimuli
negative regulation of oxidative stress−induced death
DNA−templated transcription in response to stress
regulation of response to oxidative stress
'de novo' protein folding
D
GMSC
Th17/Treg=18.21%
Prednisone
Th17/Treg=45.78%
E
Jun
Jund
Il17a
N
EAU
GMSC
Pre
F
Ccr2
Ccr6
Normal
EAU
GMSC
Prednisone
G
GMSC
Pre
GMSC up
GMSC down
common
Pre up
Gene number
-Log10q
17.5
5.0
cell activation
positive regulation of immune effector process
cellular macromolecule biosynthetic process
leukocyte activation
IL−17 signaling pathway
Phagosome
positive regulation of leukocyte differentiation
T cell activation
amide metabolic process
positive regulation of cellular
cellular response to external stimulus
regulation of adaptive immune response
cellular response to lipid
response to inorganic substance
response to oxidative stress
H
EAU DEGs
GMSC DEGs
Prednisone DEGs
macro
cdc
mono
B
pdc
neu
T
upregulated
downregulated
I
GMSC DEGs
Prednisone DEGs
germinal B
naive B
CD8n
Pro−T
NK
CD4n
neu
macro
Th17
Th1
CD8 eff
mono
Tfh
cDC
Treg
plasma B
pDC
pDC

Figure 6. GMSCs exhibited more specific rescue effect on EAU mice than prednisone

(A) UMAP embeddings of lymph node immune cells colored by cell subtypes. B, B cell; cDC, conventional dendritic cell; macro, macrophage; mono, monocytes; neu, neutrophil; pDC, plasmacytoid dendritic cell; T, T cell. Prednisone: prednisone-treated mice.

(B) UMAP embeddings of lymph node immune cells colored by origins. Normal, normalsubject; EAU, experimental autoimmune uveitis mouse; GMSC, GMSC-treated (therapeutic) mouse group; Prednisone: prednisone-treated mouse group.

(C) Left: schematic Venn diagram of rescue DEGs of GMSCs or prednisone. Right: GO analysis of common/specific rescue DEGs of T cells of GMSCs or prednisone. GMSC down: specifically downregulated GMSC rescue DEGs, common: common downregulated rescue DEGs, pre up: specifically upregulated prednisone rescue DEGs, pre down: specifically downregulated prednisone rescue DEGs. The number of commonly rescued upregulated DEGs and specifically upregulated GMSC rescue DEGs are too small for GO analysis.

(D) Pie charts of Th17/Treg ratios of GMSC-treated and prednisone-treated mice based on scRNA-seq.

(E and F) Violin plots of commonly rescued DEGs (E) or specific rescued DEGs by GMSCs (F) in Th17 cells.

(G) Left: schematic Venn diagram of rescue DEGs of GMSCs or prednisone in Th17 cells. Right: GO analysis of common/specific rescue DEGs of Th17 cells of GMSCs or prednisone. GMSC up: specifically upregulated GMSC rescue DEGs, GMSC down: specifically downregulated GMSC rescue DEGs, common: commonly downregulated rescue DEGs, pre up: specifically upregulated prednisone rescue DEGs. The number of commonly rescued upregulated DEGs and specifically downregulated GMSC rescue DEGs are too small for GO analysis.

(H) Network plots showed the cell-cell communications change between different types of immune cells based on different groups of DEGs. Lines represent cell-cell communication pairs, the thickness of the lines represents the number of intercellular ligand-receptor pairs, and the color of the lines represents that the ligand-receptor pairs are strengthened (red) or weakened (blue). The circles indicate the total number of pairs identified in each type of cells.

(I) Same as A, network plots of the changes of the cell-cell communication between 17 immune cell subtypes.

Next, we defined EAU DEGs, GMSC DEGs, and rescue DEGs in B cells and myeloid cells. The rescue ratios indicated strong rescue effects of GMSCs on naive B cells and monocytes (Figure 5C). Exploration of these rescue DEGs revealed the rescue effects of multiple TFs (*Fos*, *Jun*, and *Cebpb*), function-related genes (*Grb2*, *Tnfrsf13b*, and *Tnfrsf13c*), and immunoglobulin genes (*Iglc2* and *Iglc3*) in naive B cells (Figure 5D).[45–47] Correspondingly, GO analysis indicated that downregulated rescue DEGs of naive B cells were enriched in pathways associated with B cell functions (Figure 5E).

GMSCs induced profound rescue effects in myeloid clusters. We identified rescued function-associated genes in monocytes including *Cd69* and *Cxcr4* (Figure 5F).[41,48] GO analysis of rescue DEGs showed enrichment of downregulated rescue DEGs in T cell cytotoxicity mediation (Figure 5G). In cDCs, the expression of *Irf8*, which is known to play a central role in cDC formation, was rescued by GMSCs.[49]

Immunosuppressive specificity of GMSCs and prednisone

Next, we compared alterations in immune cell transcriptomes after GMSC or prednisone treatment. We integrated scRNA-seq data of prednisone-treated EAU mouse CDLNs from our previous study, identified seven types of immune cells, re-clustered T cells and B cells, and determined the DEGs for each subtype (Figures 6A, 6B, and S6C).[21]

Given the central role of lymphocytes in autoimmunity, we analyzed T and B cells, distinguished upregulated and downregulated rescue DEGs for GMSC or prednisone treatment, and generated a Venn diagram (Figures 6C and S6D). GO analysis indicated that both GMSCs and prednisone exhibited profound immunosuppressive effects, with common rescue DEGs enriched in Th17 function-associated pathways. More importantly, the specific downregulated rescue DEGs in the GMSC treatment were enriched in pathways associated with T and B cell functions, whereas those in prednisone treatment were enriched in metabolism-related categories. These results may indicate the specificity of the immunosuppressive functions of GMSCs compared to the general suppressive and metabolism-associated functions of prednisone.

Considering the T cell subsets, both treatments rescued the Th17:Treg ratio in EAU mice (Figures 6D and S6E). We also identified rescue DEGs of GMSC/prednisone and found that GMSCs and prednisone had similar rescue effects on TFs (*Jun* and *Jund*) and *Il17a* in Th17 cells (Figure 6E). No rescued expression of *Ccr2* and *Ccr6* was observed after prednisone treatment, suggesting that Th17 phenotype switching could result from the specific capacity of GMSCs (Figure 6F). GO analysis of rescued DEGs in Th17 cells revealed the specific rescue effect of GMSCs and the influence of prednisone on metabolic pathways (Figure 6G). We inferred that GMSCs had more specific immunosuppressive effects on T cells and prednisone had strong effects on cellular metabolic processes.

To better depict the different effects of GMSCs and prednisone, we explored the intercellular interactions between immune cells by determining the number of ligand-receptor pairs. The results indicated enhanced cell-cell communication in EAU, and GMSCs showed a stronger rescue effect than prednisone

treatment (Figure 6H). After distinguishing T cell subsets, we found that GMSC treatment strongly altered the communication between Th17 cells and other immune cells, indicating a unique effect on Th17 cells (Figure 6I). Overall, the results indicate that GMSCs showed more specific rescue effects and unique phenotype-switching capacity in EAU mice than prednisone treatment.

DISCUSSION

This study reveals the potential of GMSCs in treating AU in experimental conditions and provides a comprehensive immune cell atlas of EAU- and GMSC-treated mice. We revealed that changes in the cell type proportion, cell type-dependent gene regulation, and Th17 phenotype switching play key roles in inflammation resolution. Compared to GCs, GMSCs exhibited more specific immunosuppressive properties and a unique Th17 phenotype switching effect.

Initially isolated in 2009, GMSCs have become easily accessible and expandable sources of MSCs with similar multipotent differentiation and immunosuppressive capabilities.[7,8] Studies have demonstrated the immunosuppressive effect of GMSCs on immune systems, including suppressing T cell activation and proliferation, inducing T cell apoptosis, modulating B cell proliferation and function, and inhibiting DCs antigen presentation.[1,2,50,51] GMSCs have shown effectiveness in controlling arthritis, systemic lupus erythematosus, rheumatoid arthritis, oral mucositis, multiple sclerosis, and experimental colitis, endowing GMSCs with immunomodulatory therapeutic potentials for various autoimmune and inflammatory diseases via the suppression of T cells, B cells, and antigen-presenting cells.[50,52,53] More recently, a study focusing on the therapeutic effect of MSCs on EAU has shown their immunosuppressive properties with a reduced production of Th17 cytokines and a decreased proportion of Th17 cells after MSC treatment.[54] However, most of these studies were based on histological analysis, flow cytometry, and bulk RNA sequencing, without depiction of cell type-dependent transcriptomic changes. Consistent with the current understanding, we revealed considerable rescue effects on T cells, B cells, DCs, and monocytes, as evaluated by cell type composition. Previous studies have demonstrated that GMSCs can suppress Th17 cell development and induce Treg formation.[55,56] Consistently, among all T cell subpopulations, the study found that Th17 cells were most strongly affected by GMSCs, and that the proportion of Treg cells was elevated. Regarding transcriptomic changes, we identified rescued function-related genes by GMSCs in Th17 cells, including *Rac1* and *Rora*, which regulate Th17 function and promote Th17 differentiation, respectively.[23,24] Of interest, we also identified increased proportion of neutrophils in GMSC-treated mice, which is consistent with previous studies indicating MSCs' capability of promoting neutrophil recruitment and phagocytic activity.[57] Moreover, the similarly elevated proportion of macrophages by GMSCs, with the previous evidence that GMSCs enhance M2 polarization of macrophages, could further support the immunosuppressive properties of GMSCs.[58]

Th17 cells differ in their inflammatory potential. More recently, Kara et al. depicted a unique cell surface signature, $CCR6^{-}CCR2^{+}$ of GM-CSF-producing Th17 cells and $CCR6^{+}CCR2^{+}$ of IL-10-producing Th17 cells.[32] Validated on transcription and protein levels, our results suggested that GMSCs strongly rescued the proportion of $CCR6^{-}CCR2^{+}$ Th17 cells, and upregulated production of anti-inflammatory IL-10 in $CCR6^{+}CCR2^{+}$ Th17 cells, which could mechanistically account for GMSC effects.

GCs are among the most frequently prescribed anti-inflammatory drugs for autoimmune diseases, despite multiple side effects including osteoporosis, hyperglycemia, and GC-refractory problems.[20] To understand the different immunosuppressive capacity of GMSCs and GCs, comprehensive comparative analysis is needed. In the current study, GMSCs showed more specific rescue effects in EAU mice, including a unique Th17 phenotype switching capacity. Despite the common anti-inflammatory functions of GMSCs and GCs, the latter seemed to have an impact on the metabolic pathways of T and B lymphocytes, which could result in multiple side effects.

Overall, our results provide a single-cell expression atlas that aids in systematically annotating cell type-dependent transcriptional changes by GMSCs and elucidated Th17 phenotype switching as one of the complex mechanisms of action of GMSCs. We comprehensively compared immune cell transcriptomic changes in GMSCs and GCs, highlighting the specific immunosuppressive properties of GMSCs.

Limitations of the study

In this study, we generated a lymph node single-cell transcriptomic atlas of GMSC-treated EAU mice. An important limitation of our study was the relatively small number of sequenced samples and no validation of cell

proportion alterations after GMSC treatment. Owing to the high cost of scRNA-seq, evaluation using biological replicates is lacking. Further experimental validation is required to determine the precise position of GMSCs in EAU treatment, which could provide more information on the underlying mechanisms of GMSC therapy.

STAR★METHODS

Detailed methods are provided in the online version of this paper and include the following:

- KEY RESOURCES TABLE
- RESOURCE AVAILABILITY
  - Lead contact
  - Materials availability
  - Data and code availability
- EXPERIMENTAL MODEL AND SUBJECT DETAILS
  - EAU mouse model induction and clinical score
  - Isolation and culture of GMSCs
  - Mice treatment
- METHOD DETAILS
  - Single-cell suspension preparation
  - Flow cytometry
  - scRNA-seq and cell annotation
  - Functional enrichment analysis
  - Intercellular communication analysis
- QUANTIFICATION AND STATISTICAL ANALYSIS

SUPPLEMENTAL INFORMATION

Supplemental information can be found online at https://doi.org/10.1016/j.isci.2023.106729.

ACKNOWLEDGMENTS

Supported by the National Key Research and Development Program of China (2017YFA0105804), and the National Outstanding Youth Science Fund Project of China (8212200477).

AUTHOR CONTRIBUTIONS

W.S. and X.C.L designed the study. R.D. and Y.G. conducted the experiment and acquired the data. Y.G. analyzed the data and prepared the figures. H.L., T.T., S.Z., and X.X.L. wrote the manuscript. Z.L., L.J., and L.Z. assisted the experiments. B.C. performed the statistical analyses. The manuscript was reviewed by all authors. Order of co-first author is based on the length of time spent on the project.

DECLARATION OF INTERESTS

The authors declare no competing interests.

Received: September 3, 2022
Revised: March 22, 2023
Accepted: April 19, 2023
Published: April 23, 2023

REFERENCES

1. Weiss, A.R.R., and Dahlke, M.H. (2019). Immunomodulation by mesenchymal stem cells (MSCs): mechanisms of action of living, apoptotic, and dead MSCs. Front. Immunol. *10*, 1191. https://doi.org/10.3389/fimmu.2019.01191.

2. English, K. (2013). Mechanisms of mesenchymal stromal cell immunomodulation. Immunol. Cell Biol. *91*, 19–26. https://doi.org/10.1038/icb.2012.56.

3. Su, W., Wan, Q., Huang, J., Han, L., Chen, X., Chen, G., Olsen, N., Zheng, S.G., and Liang, D. (2015). Culture medium from TNF-alpha-stimulated mesenchymal stem cells attenuates allergic conjunctivitis through multiple antiallergic mechanisms. J. Allergy Clin. Immunol. *136*, 423–432.e8. https://doi.org/10.1016/j.jaci.2014.12.1926.

4. Dazzi, F., and Krampera, M. (2011). Mesenchymal stem cells and autoimmune diseases. Best Pract. Res. Clin. Haematol. *24*, 49–57. https://doi.org/10.1016/j.beha.2011.01.002.

5. Bernardo, M.E., and Fibbe, W.E. (2012). Safety and efficacy of mesenchymal stromal cell therapy in autoimmune disorders. Ann. N. Y. Acad. Sci. *1266*, 107–117. https://doi.org/10.1111/j.1749-6632.2012.06667.x.

6. Li, H., Tian, Y., Xie, L., Liu, X., Huang, Z., and Su, W. (2020). Mesenchymal stem cells in allergic diseases: current status. Allergol. Int.

69, 35–45. https://doi.org/10.1016/j.alit.2019.08.001.

7. Zhang, Q., Shi, S., Liu, Y., Uyanne, J., Shi, Y., Shi, S., and Le, A.D. (2009). Mesenchymal stem cells derived from human gingiva are capable of immunomodulatory functions and ameliorate inflammation-related tissue destruction in experimental colitis. J. Immunol. *183*, 7787–7798. https://doi.org/10.4049/jimmunol.0902318.

8. Fawzy El-Sayed, K.M., and Dörfer, C.E. (2016). Gingival mesenchymal stem/progenitor cells: a unique tissue engineering Gem. Stem Cells Int. *2016*, 7154327. https://doi.org/10.1155/2016/7154327.

9. Fournier, B.P.J., Larjava, H., and Häkkinen, L. (2013). Gingiva as a source of stem cells with therapeutic potential. Stem Cells Dev. *22*, 3157–3177. https://doi.org/10.1089/scd.2013.0015.

10. Zhang, X., Huang, F., Li, W., Dang, J.L., Yuan, J., Wang, J., Zeng, D.L., Sun, C.X., Liu, Y.Y., Ao, Q., et al. (2018). Human gingiva-derived mesenchymal stem cells modulate monocytes/macrophages and alleviate atherosclerosis. Front. Immunol. *9*, 878. https://doi.org/10.3389/fimmu.2018.00878.

11. El-Jawhari, J.J., El-Sherbiny, Y.M., Jones, E.A., and McGonagle, D. (2014). Mesenchymal stem cells, autoimmunity and rheumatoid arthritis. QJM *107*, 505–514.

12. Yu, Z., Wen, Y., Jiang, N., Li, Z., Guan, J., Zhang, Y., Deng, C., Zhao, L., Zheng, S.G., Zhu, Y., et al. (2022). TNF-alpha stimulation enhances the neuroprotective effects of gingival MSCs derived exosomes in retinal ischemia-reperfusion injury via the MEG3/miR-21a-5p axis. Biomaterials *284*, 121484. https://doi.org/10.1016/j.biomaterials.2022.121484.

13. Lu, Y., Xu, Y., Zhang, S., Gao, J., Gan, X., Zheng, J., Lu, L., Zeng, W., and Gu, J. (2019). Human gingiva-derived mesenchymal stem cells alleviate inflammatory bowel disease via IL-10 signalling-dependent modulation of immune cells. Scand. J. Immunol. *90*, e12751. https://doi.org/10.1111/sji.12751.

14. Wu, W., Xiao, Z.X., Zeng, D., Huang, F., Wang, J., Liu, Y., Bellanti, J.A., Olsen, N., and Zheng, S.G. (2020). B7-H1 promotes the functional effect of human gingiva-derived mesenchymal stem cells on collagen-induced arthritis murine model. Mol. Ther. *28*, 2417–2429. https://doi.org/10.1016/j.ymthe.2020.07.002.

15. Prete, M., Dammacco, R., Fatone, M.C., and Racanelli, V. (2016). Autoimmune uveitis: clinical, pathogenetic, and therapeutic features. Clin. Exp. Med. *16*, 125–136. https://doi.org/10.1007/s10238-015-0345-6.

16. Lee, R.W., Nicholson, L.B., Sen, H.N., Chan, C.C., Wei, L., Nussenblatt, R.B., and Dick, A.D. (2014). Autoimmune and autoinflammatory mechanisms in uveitis. Semin. Immunopathol. *36*, 581–594. https://doi.org/10.1007/s00281-014-0433-9.

17. Sun, D., Liang, D., Kaplan, H.J., and Shao, H. (2015). The role of Th17-associated cytokines in the pathogenesis of experimental autoimmune uveitis (EAU). Cytokine *74*, 76–80.

18. Prete, M., Dammacco, R., Fatone, M.C., and Racanelli, V. (2016). Autoimmune uveitis: clinical, pathogenetic, and therapeutic features. Clin. Exp. Med. *16*, 125–136.

19. Louveau, A., Herz, J., Alme, M.N., Salvador, A.F., Dong, M.Q., Viar, K.E., Herod, S.G., Knopp, J., Setliff, J.C., Lupi, A.L., et al. (2018). CNS lymphatic drainage and neuroinflammation are regulated by meningeal lymphatic vasculature. Nat. Neurosci. *21*, 1380–1391. https://doi.org/10.1038/s41593-018-0227-9.

20. Timmermans, S., Souffriau, J., and Libert, C. (2019). A general introduction to glucocorticoid biology. Front. Immunol. *10*, 1545. https://doi.org/10.3389/fimmu.2019.01545.

21. Li, H., Gao, Y., Xie, L., Wang, R., Duan, R., Li, Z., Chen, B., Zhu, L., Wang, X., and Su, W. (2021). Prednisone reprograms the transcriptional immune cell landscape in CNS autoimmune disease. Front. Immunol. *12*, 739605.

22. Campos-Mora, M., Contreras-Kallens, P., Gálvez-Jirón, F., Rojas, M., Rojas, C., Refisch, A., Cerda, O., and Pino-Lagos, K. (2019). CD4+Foxp3+T regulatory cells promote transplantation tolerance by modulating effector CD4+ T cells in a neuropilin-1-dependent manner. Front. Immunol. *10*, 882. https://doi.org/10.3389/fimmu.2019.00882.

23. Kurdi, A.T., Bassil, R., Olah, M., Wu, C., Xiao, S., Taga, M., Frangieh, M., Buttrick, T., Orent, W., Bradshaw, E.M., et al. (2016). Tiam1/Rac1 complex controls Il17a transcription and autoimmunity. Nat. Commun. *7*, 13048.

24. McAleer, J.P., and Kolls, J.K. (2011). Mechanisms controlling Th17 cytokine expression and host defense. J. Leukoc. Biol. *90*, 263–270.

25. Chen, H., Xu, X., Teng, J., Cheng, S., Bunjhoo, H., Cao, Y., Liu, J., Xie, J., Wang, C., and Xu, Y. (2016). CXCR4 inhibitor attenuates ovalbumin-induced airway inflammation and hyperresponsiveness by inhibiting Th17 and Tc17 cell immune response. Exp. Ther. Med. *11*, 1865–1870.

26. Hirata, T., Osuga, Y., Takamura, M., Kodama, A., Hirota, Y., Koga, K., Yoshino, O., Harada, M., Takemura, Y., Yano, T., and Taketani, Y. (2010). Recruitment of CCR6-expressing Th17 cells by CCL 20 secreted from IL-1 beta-TNF-alpha-and IL-17A-stimulated endometriotic stromal cells. Endocrinology *151*, 5468–5476. https://doi.org/10.1210/en.2010-0398.

27. Langrish, C.L., Chen, Y., Blumenschein, W.M., Mattson, J., Basham, B., Sedgwick, J.D., McClanahan, T., Kastelein, R.A., and Cua, D.J. (2005). IL-23 drives a pathogenic T cell population that induces autoimmune inflammation. J. Exp. Med. *201*, 233–240.

28. Codarri, L., Gyülvészi, G., Tosevski, V., Hesske, L., Fontana, A., Magnenat, L., Suter, T., and Becher, B. (2011). RORγt drives production of the cytokine GM-CSF in helper T cells, which is essential for the effector phase of autoimmune neuroinflammation. Nat. Immunol. *12*, 560–567.

29. McGeachy, M.J., Bak-Jensen, K.S., Chen, Y., Tato, C.M., Blumenschein, W., McClanahan, T., and Cua, D.J. (2007). TGF-β and IL-6 drive the production of IL-17 and IL-10 by T cells and restrain TH-17 cell–mediated pathology. Nat. Immunol. *8*, 1390–1397.

30. Ghoreschi, K., Laurence, A., Yang, X.-P., Tato, C.M., McGeachy, M.J., Konkel, J.E., Ramos, H.L., Wei, L., Davidson, T.S., Bouladoux, N., et al. (2010). Generation of pathogenic TH17 cells in the absence of TGF-β signalling. Nature *467*, 967–971.

31. Haines, C.J., Chen, Y., Blumenschein, W.M., Jain, R., Chang, C., Joyce-Shaikh, B., Porth, K., Boniface, K., Mattson, J., Basham, B., et al. (2013). Autoimmune memory T helper 17 cell function and expansion are dependent on interleukin-23. Cell Rep. *3*, 1378–1388.

32. Kara, E.E., McKenzie, D.R., Bastow, C.R., Gregor, C.E., Fenix, K.A., Ogunniyi, A.D., Paton, J.C., Mack, M., Pombal, D.R., Seillet, C., et al. (2015). CCR2 defines in vivo development and homing of IL-23-driven GM-CSF-producing Th17 cells. Nat. Commun. *6*, 8644. https://doi.org/10.1038/ncomms9644.

33. Yu, X., Teng, X.-L., Wang, F., Zheng, Y., Qu, G., Zhou, Y., Hu, Z., Wu, Z., Chang, Y., Chen, L., et al. (2018). Metabolic control of regulatory T cell stability and function by TRAF3IP3 at the lysosome. J. Exp. Med. *215*, 2463–2476.

34. Li, Z., Lin, F., Zhuo, C., Deng, G., Chen, Z., Yin, S., Gao, Z., Piccioni, M., Tsun, A., Cai, S., et al. (2014). PIM1 kinase phosphorylates the human transcription factor FOXP3 at serine 422 to negatively regulate its activity under inflammation. J. Biol. Chem. *289*, 26872–26881.

35. Wojciechowski, S., Tripathi, P., Bourdeau, T., Acero, L., Grimes, H.L., Katz, J.D., Finkelman, F.D., and Hildeman, D.A. (2007). Bim/Bcl-2 balance is critical for maintaining naive and memory T cell homeostasis. J. Exp. Med. *204*, 1665–1675.

36. Carrington, E.M., Zhan, Y., Brady, J.L., Zhang, J.-G., Sutherland, R.M., Anstee, N.S., Schenk, R.L., Vikstrom, I.B., Delconte, R.B., Segal, D., et al. (2017). Anti-apoptotic proteins BCL-2, MCL-1 and A1 summate collectively to maintain survival of immune cell populations both in vitro and in vivo. Cell Death Differ. *24*, 878–888.

37. Ahlfors, H., Limaye, A., Elo, L.L., Tuomela, S., Burute, M., Gottimukkala, K.V.P., Notani, D., Rasool, O., Galande, S., and Lahesmaa, R. (2010). SATB1 dictates expression of multiple genes including IL-5 involved in human T helper cell differentiation. Blood *116*, 1443–1453.

38. Riella, L.V., Paterson, A.M., Sharpe, A.H., and Chandraker, A. (2012). Role of the PD-1 pathway in the immune response. Am. J. Transplant. *12*, 2575–2587.

39. Robertson, M.J. (2002). Role of chemokines in the biology of natural killer cells. J. Leukoc. Biol. *71*, 173–183. https://doi.org/10.1189/jlb.71.2.173.

40. Fehniger, T.A., Cai, S.F., Cao, X., Bredemeyer, A.J., Presti, R.M., French, A.R., and Ley, T.J. (2007). Acquisition of murine NK cell cytotoxicity requires the translation of a pre-existing pool of granzyme B and perforin mRNAs. Immunity *26*, 798–811.

41. Sancho, D., Gómez, M., and Sánchez-Madrid, F. (2005). CD69 is an immunoregulatory molecule induced following activation. Trends Immunol. *26*, 136–140.

42. Basha, G., Omilusik, K., Chavez-Steenbock, A., Reinicke, A.T., Lack, N., Choi, K.B., and Jefferies, W.A. (2012). A CD74-dependent MHC class I endolysosomal cross-presentation pathway. Nat. Immunol. *13*, 237–245.

43. Clambey, E.T., McNamee, E.N., Westrich, J.A., Glover, L.E., Campbell, E.L., Jedlicka, P., De Zoeten, E.F., Cambier, J.C., Stenmark, K.R., and Colgan, S.P. (2012). Hypoxia-inducible factor-1 alpha–dependent induction of FoxP3 drives regulatory T-cell abundance and function during inflammatory hypoxia of the mucosa. Proc. Natl. Acad. Sci. USA *109*, E2784–E2793.

44. Golovina, T.N., Mikheeva, T., Suhoski, M.M., Aqui, N.A., Tai, V.C., Shan, X., Liu, R., Balcarcel, R.R., Fisher, N., Levine, B.L., et al. (2008). CD28 costimulation is essential for human T regulatory expansion and function. J. Immunol. *181*, 2855–2868.

45. Ackermann, J.A., Radtke, D., Maurberger, A., Winkler, T.H., and Nitschke, L. (2011). Grb2 regulates B-cell maturation, B-cell memory responses and inhibits B-cell Ca2+ signalling. EMBO J. *30*, 1621–1633.

46. Figgett, W.A., Fairfax, K., Vincent, F.B., Le Page, M.A., Katik, I., Deliyanti, D., Quah, P.S., Verma, P., Grumont, R., Gerondakis, S., et al. (2013). The TACI receptor regulates T-cell-independent marginal zone B cell responses through innate activation-induced cell death. Immunity *39*, 573–583.

47. Smulski, C.R., and Eibel, H. (2018). BAFF and BAFF-receptor in B cell selection and survival. Front. Immunol. *9*, 2285.

48. Werner, Y., Mass, E., Ashok Kumar, P., Ulas, T., Händler, K., Horne, A., Klee, K., Lupp, A., Schütz, D., Saaber, F., et al. (2020). Cxcr4 distinguishes HSC-derived monocytes from microglia and reveals monocyte immune responses to experimental stroke. Nat. Neurosci. *23*, 351–362.

49. Sichien, D., Scott, C.L., Martens, L., Vanderkerken, M., Van Gassen, S., Plantinga, M., Joeris, T., De Prijck, S., Vanhoutte, L., Vanheerswynghels, M., et al. (2016). IRF8 transcription factor controls survival and function of terminally differentiated conventional and plasmacytoid dendritic cells, respectively. Immunity *45*, 626–640.

50. Chen, M., Su, W., Lin, X., Guo, Z., Wang, J., Zhang, Q., Brand, D., Ryffel, B., Huang, J., Liu, Z., et al. (2013). Adoptive transfer of human gingiva-derived mesenchymal stem cells ameliorates collagen-induced arthritis via suppression of Th1 and Th17 cells and enhancement of regulatory T cell differentiation. Arthritis Rheum. *65*, 1181–1193. https://doi.org/10.1002/art.37894.

51. Zhao, J., Chen, J., Huang, F., Wang, J., Su, W., Zhou, J., Qi, Q., Cao, F., Sun, B., Liu, Z., et al. (2019). Human gingiva tissue-derived MSC ameliorates immune-mediated bone marrow failure of aplastic anemia via suppression of Th1 and Th17 cells and enhancement of CD4+Foxp3+ regulatory T cells differentiation. Am. J. Transl. Res. *11*, 7627–7643.

52. Zhang, X., Huang, F., Li, W., Dang, J.-l., Yuan, J., Wang, J., Zeng, D.-L., Sun, C.-X., Liu, Y.-Y., Ao, Q., et al. (2018). Human gingiva-derived mesenchymal stem cells modulate monocytes/macrophages and alleviate atherosclerosis. Front. Immunol. *9*, 878.

53. Kim, D., Lee, A.E., Xu, Q., Zhang, Q., and Le, A.D. (2021). Gingiva-derived mesenchymal stem cells: potential application in tissue engineering and regenerative medicine-a comprehensive review. Front. Immunol. *12*, 667221.

54. Mu, Y., Xu, W., Liu, J., Wang, Y., Chen, J., and Zhou, Q. (2022). Mesenchymal stem cells moderate experimental autoimmune uveitis by dynamic regulating Th17 and Breg cells response. J. Tissue Eng. Regen. Med. *16*, 26–35.

55. Tatara, R., Ozaki, K., Kikuchi, Y., Hatanaka, K., Oh, I., Meguro, A., Matsu, H., Sato, K., and Ozawa, K. (2011). Mesenchymal stromal cells inhibit Th17 but not regulatory T-cell differentiation. Cytotherapy *13*, 686–694.

56. Engela, A.U., Baan, C.C., Dor, F.J.M.F., Weimar, W., and Hoogduijn, M.J. (2012). On the interactions between mesenchymal stem cells and regulatory T cells for immunomodulation in transplantation. Front. Immunol. *3*, 126.

57. Joel, M.D.M., Yuan, J., Wang, J., Yan, Y., Qian, H., Zhang, X., Xu, W., and Mao, F. (2019). MSC: immunoregulatory effects, roles on neutrophils and evolving clinical potentials. Am. J. Transl. Res. *11*, 3890–3904.

58. François, M., Romieu-Mourez, R., Li, M., and Galipeau, J. (2012). Human MSC suppression correlates with cytokine induction of indoleamine 2, 3-dioxygenase and bystander M2 macrophage differentiation. Mol. Ther. *20*, 187–195.

59. Agarwal, R.K., Silver, P.B., and Caspi, R.R. (2012). Rodent models of experimental autoimmune uveitis. In Autoimmunity (Springer), pp. 443–469.

60. Chen, J., and Caspi, R.R. (2019). Clinical and functional evaluation of ocular inflammatory disease using the model of experimental autoimmune uveitis. In Immunological Tolerance (Springer), pp. 211–227.

61. Ko, J.H., Lee, H.J., Jeong, H.J., Kim, M.K., Wee, W.R., Yoon, S.O., Choi, H., Prockop, D.J., and Oh, J.Y. (2016). Mesenchymal stem/stromal cells precondition lung monocytes/macrophages to produce tolerance against allo- and autoimmunity in the eye. Proc. Natl. Acad. Sci. USA *113*, 158–163. https://doi.org/10.1073/pnas.1522905113.

62. Butler, A., Hoffman, P., Smibert, P., Papalexi, E., and Satija, R. (2018). Integrating single-cell transcriptomic data across different conditions, technologies, and species. Nat. Biotechnol. *36*, 411–420.

63. Zhou, Y., Zhou, B., Pache, L., Chang, M., Khodabakhshi, A.H., Tanaseichuk, O., Benner, C., and Chanda, S.K. (2019). Metascape provides a biologist-oriented resource for the analysis of systems-level datasets. Nat. Commun. *10*, 1523.

64. Ginestet, C. (2011). ggplot2: elegant graphics for data analysis. J. Roy. Stat. Soc. *174*, 245–246.

65. Sergushichev, A. (2016). An algorithm for fast preranked gene set enrichment analysis using cumulative statistic calculation. Preprint at bioRxiv. https://doi.org/10.1101/060012.

66. Efremova, M., Vento-Tormo, M., Teichmann, S.A., and Vento-Tormo, R. (2020). CellPhoneDB: inferring cell–cell communication from combined expression of multi-subunit ligand–receptor complexes. Nat. Protoc. *15*, 1484–1506.

STAR★METHODS

KEY RESOURCES TABLE

REAGENT or RESOURCE	SOURCE	IDENTIFIER
Antibodies		
Zombie NIR	Biolegend	423106
CD4	Biolegend	100434
IL17A	Biolegend	506912
CCR6	Biolegend	129819
CCR2	Biolegend	150621
GM-CSF	Biolegend	505411
IL10	Biolegend	505008
CD45	Biolegend	103138
CD45	Biolegend	304027
CD34	Biolegend	343607
CD44	eBioscience	17-0441-82
CD90	Biolegend	328121
CD73	eBioscience	12-0739-42
CD105	eBioscience	12-1057-42
CD39	eBioscience	11-0399-42
HLA-DR	eBioscience	11-9952-41
CD29	eBioscience	11-0299-42
CD14	Biolegend	301803
CD19	Biolegend	115543
CD3ε	Biolegend	100307
CD25	Biolegend	102016
PD-1	Biolegend	135206
CXCR5	Biolegend	145505
B220	Biolegend	103248
IFN-γ	Biolegend	505808
Foxp3	eBioscience	11-5773-82
Biological samples		
GMSC	Third Hospital at the Sun Yat-sen University	IRB 2018-02-195-01
Chemicals, peptides, and recombinant proteins		
IRBP1-20	GiL Biochem	051038
complete Freund's adjuvant	BD Difco	SLCC1714
Mycobacterium tuberculosis strain H37Ra	BD Difco	1294163
BFA	Sigma-Aldrich	059M4011V
Ion	Sigma-Aldrich	3484188
PTX	Sigma-Aldrich	180242A1
PMA	Sigma-Aldrich	MKCG6950
Deposited data		
Raw data	This paper	GSA: HRA002422, GSA: HRA000850
Code for downstream analysis	This paper	https://github.com/panpipe1997/code-for-GMSC-treated-EAU-scRNA-seq/tree/main

(*Continued on next page*)

Continued

REAGENT or RESOURCE	SOURCE	IDENTIFIER
Experimental models: Organisms/strains		
Mouse:C57BL/6j	Guangzhou Animal Testing Center	N/A
Software and algorithms		
FlowJo software	FlowJo Co.	N/A
Other		
Micron IV fundus camera	Phoenix Co.	N/A
BD LSRFortessa instrument	BD Biosciences	N/A

RESOURCE AVAILABILITY

Lead contact

Further information and request for resources and reagents should be directed to and will be fulfilled by the lead contact, Wenru Su (suwr3@mail.sysu.edu.cn).

Materials availability

The study did not generate new unique reagents.

Data and code availability

- Single-cell RNA-seq data have been deposited at Genome Sequence Archive (GSA) and are publicly available as of the date of publication. Accession numbers: HRA002422 (GSA), HRA000850 (GSA). Code for downstream analysis can be found here: https://github.com/panpipe1997/code-for-GMSC-treated-EAU-scRNA-seq.
- This paper does not report original code.
- Any additional information required to reanalyze the data reported in this paper is available from the lead contact upon request.

EXPERIMENTAL MODEL AND SUBJECT DETAILS

EAU mouse model induction and clinical score

Guangzhou Animal Testing Center offered 6-8 weeksold female C57BL/6J mice (18-25g). All experiments were conducted in accordance with the policies for animal health and usage. Animal experiments were allowed by the Institutional Animal Care Committee (Zhongshan Ophthalmic Center, Sun Yat-Sen University). Mice received subcutaneous injection of a 1:1 volume ratio of emulsion with 2 mg/mL of human interphotoreceptor retinoid-binding protein 1-20 ($IRBP_{1-20}$, GPTHLFQPSLVLDMAKVLLD, GiL Biochem, Shanghai, China), complete Freund's adjuvant (BD Difco, San Jose, CA, USA) with 2.5 mg of *Mycobacterium tuberculosis* strain H37Ra (BD Difco, San Jose, CA, USA). All mice were housed in pathogen free environment.[59,60] Each mouse was injected with 200 ul emulsion totally, 100 ul at the back spot, 50 ul near the tail and two flanks, separately. Additionally, mice received intraperitoneal injection of 0.25 μg pertussis toxin (Sigma-Aldrich, St. Louis, MO, USA) on the same day and 2 days after immunization. The Micron IV fundus camera (Phoenix Co., Campbell, CA, USA) was utilized to observe mice fundus, and clinical score was graded from 0 to 4 scoring.[60] A total of 18 female mice will be needed. Data will be analyzed using a one-way ANOVA with a type I error level of 5%. We assumed that clinical scores would result 14 days after GMSC treatment. Based on those data, along with the previous researches, six mice would satisfy the need of the current study.

Isolation and culture of GMSCs

All procedures of GMSC isolation and culture were approved by the medical ethics committees of Institutional Review Boards (IRB) in the Third Hospital at the Sun Yat-sen University (IRB 2018-02-195-01). Human gingiva samples were collected from discarded tissues of four healthy individuals who had no history of periodontal disease and relatively healthy periodontium, during routine dental procedures at the Division of Dentistry in the Third Hospital at the Sun Yat-sen University. After digesting gingiva tissues with dispase II (2 mg/mL, 37°C for 2 h) and collagenase IV (4 mg/mL, 37°C for 0.5 h), we filtered the gingiva cell suspension

with a 70-μm cells trainer and centrifuged it. Then we re-suspended the cells and transferred them to a 10 cm dish containing 10% fetal bovine serum, 100 U/mL penicillin/100 μg/mL streptomycin. The cells were incubated with 5% CO2 and 95% O2. Then, we collected the plastic-adherent GMSCs. Finally, we examined the GMSCs with human mAbs by flow cytometry. GMSC markers including CD14, CD29, CD39, CD105, CD73, CD90, CD44, CD34, CD45 and HLA-DR.

Mice treatment

Human gingiva-derived MSCs were provided by the Dental Division of the Third Affiliated Hospital at Sun Yat-sen University, and cultured in MEM alpha medium supplemented with 10% fetal bovine serum and 1% penicillin-streptomycin. After washing two times, the cells were resuspended in PBS at a concentration of 5 x 10^6/ml for injection *in vivo*.[61] EAU mice were administered with 2 x 10^6 cells via the tail vein at day 0 (prophylactic group) or day 7 (therapeutic group).

METHOD DETAILS

Single-cell suspension preparation

Single-cell suspension was prepared from neck CDLNs with filtration through 70-μm strainers (352235, Falcon). Cells viability in each sample exceeded 85% after two times of washing.

Flow cytometry

We isolated cells from CDLNs and stained them with live/dead dye (Thermo Fisher Scientific, Waltham, MA, USA). After that, we stained the cells with following anti-mouse surface markerCD45, CD19, CD3, CD25, PD1, CXCR5, B220 CCR6, CD4 CCR2. Cells were stimulated with 1 mg/ml BFA (Brefeldin A, Sigma), 5 ng/ml PMA (Phorbol 12-Myristate 13-Acetate, Sigma), and 0.5 mg/ml Ion (Sigma) at 37°C for 4-5 h and then further fixated and permeabilized. Then, the cells were stained with IFN-y, Foxp3, GM-CSF, IL10, IL-17a. These stained cells were analyzed via BD LSRFortessa instrument (BD Biosciences). FlowJo software 10.0 (FlowJo Co., OR, USA) was utilized to evaluate data.

scRNA-seq and cell annotation

CDLNs from three groups were mixed and sequenced (three mice per group). For library generation, scRNA-seq reagent kit (10x Genomics) was used. CellRanger (ver 5.0.0) was used to process sequencing data. Data integration and clustering was based on Seurat (ver 4.0.5).[62] Cells with <200 genes, >2500 genes or mitochondrial gene ratio >10% were filtered out.

Seurat "FindAllMarkers()" function was utilized to identify genes with higher expression in each cell subpopulation with default parameters. Briefly, we first annotate T cells with the expression of *Cd3d, Cd3e, Cd3g* and *Il7r*; we annotate B cells with *Cd79a, Cd79b, Ms4a1* and *Mzb1*; we annotate conventional dendritic cells with *Ly6c2* and *Ccl22*; we annotate monocytes with *Ccr2* and *Ifitm3*; we annotate macrophages with *Apoe, C1qa* and *C1qb*; we annotate neutrophils with *S100a9, Lcn2, Anxa1* and *Il1b*; we annotate plasmacytoid dendritic cells with *Siglech, Cox6a2, Irf8* and *Tcf4*.

For T cell subpopulations, we annotate Th17 cells with the expression of *Il17a, Ccr2*, and *Ly6a*; we annotate proliferating T cells with *Hmgb2, Mki67* and *Stmn1*; we annotate regulatory T cells with *Foxp3* and *Il2ra*; we annotate $CD4^+$ naïve T cells with *Cd4, Ccr7* and *Igfbp4*; we annotate $CD8^+$ naïve T cells with *Cd8a, Cd8b*, and *Nkg7*; we annotate $CD8^+$ effector T cells with *Cd8a, Ccl5* and *Cxcr3*; we annotate NK cells with *Gzmb, Ncr1* and *Gzma*. Th1 and Tfh cells both expressed higher levels of *Ifngr1, Cd40lg* and *Sh2d1a*, and these two subpopulations were further distinguished by sub-clustering with expression of *Tcf7, Lgals3* and *Cxcr6*. Also, B cells were classified into three clusters with expression of *Mzb1, Ms4a1* and *Xbp1* for plasma B cells, expression of *H2afx, Birc5* and *Stmn1* for germinal B cells, and expression of *Cd79a, Cd79b*, and *Sell* for naïve B cells. Seurat 'FindMarkers()' function was utilized to calculate differentially expressed genes (DEGs) with Wilcoxon Rank Sum test. All genes with the following criteria were selected: (1) logfold change >0.25, (2) Adjusted p-value <0.05, (3) >5% of cells in either test group. Adjusted p-value was calculated with Bonferroni correction using all features in the dataset.

Functional enrichment analysis

Metascape (www.metascape.org) was utilized to perform gene ontology (GO) enrichment analysis.[63] The Benjamini-Hochberg procedure was used to compute q-values. GO terms or pathways in the top 50

enriched categories were graphed with ggplot2.[64] The fGSEA package was used to perform gene set enrichment analysis (GSEA), with the Kyoto Encyclopedia of Genes and Genomes gene set of MSigDB as reference.[65]

Intercellular communication analysis

CellPhoneDB software (version 1.1.0) was used to compute cell-cell communication.[66] We only analyzed ligand-receptor pairs expressed by more than 10% cells in the specific cluster with detectable ligands and receptors. We compared the average expression of each pair. CellPhoneDB provides explicit threshold (premutation-based P values) to control for false positive interaction predictions. Pairs ($P < 0.05$) were selected and graphed.

QUANTIFICATION AND STATISTICAL ANALYSIS

GraphPad Prism Software was utilized. Mean ± SD are presented in figures. P-values are generated by one-way ANOVA, followed by Kruskal-Wallis with Dunn's post-hoc test. P values above 0.05 were considered not significant. N, not significant, *$P < 0.05$, **$P < 0.01$, ***$P < 0.001$, ****$P < 0.0001$.